Computer Simulation of Sputtering

By Mark T. Robinson
Solid State Division, Oak Ridge National Laboratory
Oak Ridge, Tennessee 37831-6032, USA

Synopsis

In 1986, H. H. Andersen reviewed attempts to understand sputtering by computer simulation and identified several areas where further research was needed: potential-energy functions for molecular-dynamics modelling; the role of inelastic effects on sputtering, especially near the target surface; the modelling of surface binding in models based on the binary-collision approximation; aspects of cluster emission in molecular-dynamics models; and angular distributions of sputtered particles. To these may be added kinetic-energy distributions of sputtered particles and the relationships between molecular-dynamics and binary-collision models, as well as the development of intermediate models. Many of these topics are discussed. Recent advances in binary-collision modelling include the explicit evaluation of the time in strict binary-collision codes and the development of intermediate codes able to simulate certain many-particle problems realistically. Developments in molecular-dynamics modelling include the wide-spread use of many-body potentials in sputtering calculations, inclusion of realistic electron excitation and electron-phonon interactions, and several studies of cluster-ion impacts on solid surfaces.

Contents

1 Introduction

Computer simulation has long been an important tool in studying the complex interactions of energetic ions with condensed matter which underlie such physical processes as particle reflection (backscattering) and penetration, ion implantation, radiation damage, and target erosion (sputtering). These are processes important to such technologies as controlled fission and fusion power generation, laser isotope separation, semiconductor device manufacture, plasma processing, and others. Moreover, they are the basis for the use of ion beams in more narrowly scientific areas, such as secondary-ion mass spectrometry, surface structure determination, the location of defects and impurities in solids, and so on. For these and other reasons, the interactions of ions with solids have been studied for many years by experimental, theoretical, and computational techniques.

The methods of computational physics are useful for the direct simulation of experiments, but also supply important tools for testing the assumptions of analytical theory. In addition, the computational physicist has an almost unlimited access to the atomistic details, the mechanisms whereby the initial disturbances are linked to experimental observables. The elucidation of these mechanisms is an important objective of computer simulation.

At the conference on sputtering in Spitz an der Donau, Austria, in 1986, H. H. Andersen (1987) presented a critical review of the status of the computer simulation of atomic collisions in solids, with a special emphasis on sputtering. Besides giving an admirably balanced and objective view of the state of the art at the time, Andersen pointed to a number of topics in need of further study. It is my purpose to examine the progress made in the past few years in addressing topics which he highlighted. A comprehensive review of the literature is not attempted: for this and for reviews of the subject from a variety of viewpoints, consult Robinson (1981), Yurasova & Eltekov (1982), Harrison (1983, 1988), Andersen (1987), Sigmund (1987b), Biersack (1987), Dodson (1989), Mashkova & Molchanov (1989), Barrett (1990), Eckstein (1991), and Smith & Webb (1992). These cover the literature rather completely up to about 1991.

This review is restricted to the low-dose sputtering of single-component targets under circumstances where atomic ejection is not a result of electron excitation effects. For a review of the electronic sputtering of inorganic insulators, see the companion article by Johnson & Schou (1993).

2 Recent Developments in Computer Hardware

Since 1986 there have been dramatic changes in computer hardware, which greatly alter the prospects for computer simulation. The developments include the introduction of scientific workstations which put what was once supercomputer power on (or next to) the desktop and major advances in parallel computing. Such developments make vector processors of the Cray type obsolete and revolutionize the environment in which simulation is done. Many of the controversies of the past are no longer interesting, since they can now be addressed in a simple manner by direct computation instead of by mere argument.

Several manufacturers have introduced machines based on so-called reduced-instruction-set computing (RISC). Using a simplified repertoire of commands, such machines achieve much higher speeds than were common heretofore. Moreover, manufacturing improvements make the new systems available at startlingly low cost and eliminate significant constraints on computer memory. To illustrate, Table 1 shows the time required by a set of MARLOWE (Robinson & Torrens 1974, Robinson 1989) test problems on some contemporary machines (Robinson 1992a). The IBM RISC System/6000, Model 320H, costs little enough in typical configurations that it can be viewed as a single-user workstation. Some models in this series support up to 512 megabytes of memory. The Cray X-MP, costing many times more, is less than twice as fast on MARLOWE and cannot compete in cost effectiveness. The situation depends strongly on the individual program, but few codes

Table 1: MARLOWE Test Problem Execution Times on Comtemporary Computers (Robinson 1992c)

Computer	Time (seconds)[a]
Cray X-MP 14	270
IBM RISC System/6000	
Model 320H	444
Model 560	222
Hewlett-Packard HP/9000	
Model 730	223
Digital VAX 6420	1141
IBM 3090-150E	458

[a] The time is the total for a set of 14 test problems

are likely to achieve time reductions exceeding five merely through vectorization.

A closely related development is the introduction of 'massively parallel' machines, such as the CM-5 from Thinking Machines Corp. and the Paragon from Intel. The former, a so-called SIMD (single instruction multiple data) machine, may be thought of as an extension of vectorization to a level a hundred times that of a Cray. The latter, an MIMD (multiple instruction multiple data) machine, resembles a network of workstation class machines, each operating more-or-less autonomously on parts of a complex task and communicating among each other by passing messages. It is also possible to use an actual network of workstations as a parallel-computing environment.

The challenging tasks are to identify the architecture appropriate to each computational application and to construct programs that use the architecture efficiently in solving the problem. Parallel computing is not simply an extension of previous practices, but, like vector processing, demands new computational techniques and new ways of formulating problems. Work on parallel implementations of classical-dynamical models is well-advanced at several institutions. It will be interesting to see these developments come to fruition in studies of (for example) sputtering in the next few years.

3 Computer Simulation Models

A rather complete list of the programs used to simulate sputtering processes is given in the report of a round-robin collaboration (Sigmund et al. 1989). It is difficult to

develop a fully satisfying taxonomy of such codes for each has characteristic features which differentiate it from nominally similar ones. However, for the purposes of this review, four main categories of model are identified: the scheme and the notation used are those of the round-robin report.

First are codes which integrate the classical equations of motion of a large number of particles simultaneously, commonly called molecular-dynamics (MD) models. They are used widely in physics; for reviews, see Abraham (1986), Hoover (1986), and Allen & Tildesley (1987), among others. The best-known MD models for sputtering applications are those of D. E. Harrison, Jr. (Harrison 1983, 1988, Harrison & Jakas 1986a). The hallmark of the MD models used to simulate atomic-collision processes is that they integrate the equations of motion of many atoms until the energy added in an initial disturbance is dissipated or until some other condition is met. Various sorts of boundary conditions are used: cyclic, dissipative, fixed, free, and so on. Two-body interaction potentials were used originally, but several groups now use many-body potentials. Inelastic effects may be included. The MD models are particularly effective in working out detailed mechanisms. Questions still remain, however, about the sizes of the numerical crystallites required (event containment) and about the statistics of such calculations. Nieminen (1993) discusses the present status and future prospects of molecular-dynamics modelling.

Next are two sorts of codes using the binary-collision approximation (BCA) to solve the equations of motion of projectiles which are assumed to interact with the target atoms one at a time. This is appropriate at high kinetic energies, but breaks down at low ones. The two types of BCA codes are differentiated by the structures of the solid targets. In one group, as in the MD codes, the target has a definite structure: these are termed BC models. Besides conserving energy and momentum, such codes also conserve particles (as do MD codes), since it is easy to arrange that target sites emit only one atom. The principal example of BC codes is MARLOWE (Robinson 1989, 1992a). Such BC programs may provide an approximate treatment of overlapping collisions which occur at nearly the same time, designed to preserve the crystal symmetry which often accompanies them (Robinson 1989, 1993).

Aleatory (stochastic) methods are used in the second group of BCA codes to determine the locations of target atoms, to select impact parameters or scattering angles, and so forth. In general, such Monte Carlo (MC) codes conserve energy and momentum in single collisions, but do not conserve the number of particles. The targets are structureless: there are no correlations between the positions of target atoms except those imposed by the density of the substance. The principal examples of such programs are the family of TRIM codes (Biersack 1987).

There is unfortunate confusion in the literature between the two kinds of BCA codes, in part a result of the habit of some writers of referring improperly to the

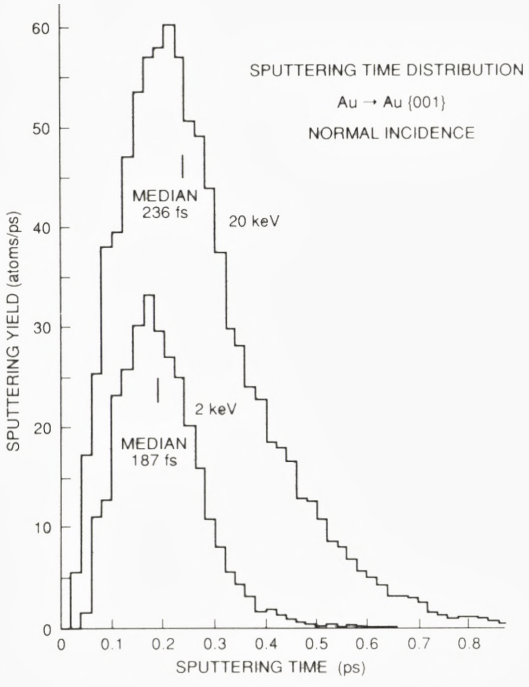

Figure 1. The distribution of sputtering times for 2 keV and 20 keV Au atoms, normally incident on Au {001} surfaces (Robinson 1992c). The potential is the Molière potential used earlier (Robinson 1992b). The median ejection times are indicated. The reference plane for the sputtering time was located 0.253 nm (0.62 of the lattice constant) in front of the target surface.

BC models as 'Monte Carlo' codes. Contrary to some statements (see, for example, Harrison & Jakas 1986a, Harrison 1988, Dodson 1990), aleatory methods play no part in determining target atom locations, impact parameters, scattering angles, and the like, in BC programs like MARLOWE.

In general, BCA codes (both BC and MC types) ignore the temporal aspects of cascade development, but it was shown recently (Robinson 1989) that the time of a collision may be evaluated explicitly in such codes, a result used to modify MARLOWE so that collisions are correctly ordered in time (Robinson 1990, 1992b, 1993). It is thus possible for BC codes to calculate things which had been thought of as the sole province of MD codes. To illustrate, Fig. 1 shows sputtering-time distributions obtained with MARLOWE for the self-sputtering of gold at two initial

kinetic energies (Robinson 1992c). The histograms are similar to those reported by Harrison (1988) for other systems. The median ejection times for Au are a little greater than he reported for Cu and Rh, mainly because of the greater mass of Au. Other MARLOWE studies of temporal aspects of sputtering are reported elsewhere (Hou et al. 1993).

There are also codes of intermediate type, combining aspects of MD models with those of BCA models. Yamamura describes two interesting models of this type: one is the 'dynamic' MC code DYACAT (Yamamura 1982, 1988, 1990, 1991), based on the earlier MC program ACAT (Takeuchi & Yamamura 1983); the other is the 'dynamic' BC code DYACOCT (Yamamura et al. 1989), based on the BC program ACOCT (Yamamura & Takeuchi 1987). Both codes include collisions between moving projectiles and keep track of the time properly. At each encounter, they locate the potential target atom for which the collision time is least and a collision diameter is derived from the parameters of this encounter. If only one target is found within the collision diameter, the BCA is applied in the usual way, including the necessary modifications for moving target atoms. However, if several targets are present, the codes integrate the equations of motion of the entire group of particles, including the interactions of the projectile with all targets, but ignoring the interactions of the targets with each other. With these modifications, Yamamura's codes remain comparatively fast, but are still able to deal with many situations where MD codes were previously required. For example, DYACAT was used to study cluster bombardments (Yamamura 1990, 1991).

The QDYN program (Harrison & Jakas 1986a) is also an intermediate code, but one much closer to full MD models than are Yamamura's. The motion of an atom is ignored until it is struck by an already moving atom with a force exceeding a minimum value. This feature resembles aspects of quasistable MD codes (Schlaug 1966, Torrens 1973, Schwartz et al. 1976, Heinisch et al. 1979), although the older programs used energy criteria instead. In either case, completeness in the model is surrendered to achieve speed.

An alternative procedure for accelerating MD calculations is to truncate the interaction potential severely, including only repulsive forces between atoms separated by less than the equilibrium nearest-neighbor distance in the target, and adjusting matters so that there is no force between atoms on their equilibrium sites. Such metastable MD models permit quite speedy calculations and were once widely used (see Robinson 1981 for references), but their lack of restoring forces restricts them to problems in which the equilibrium state is not important. A recent example of such a code is that of Shulga (1991).

Hybrid codes are also possible. For example, Webb et al. (1986) describe QDRIM, a code which combines a TRIM-like treatment of deeply penetrating particles with a QDYN treatment of the region near the surface. Another hybrid

approach is that of Pan & Hou (1992), who used MARLOWE for the collisional phase of cascade development and an MD model to follow the aging of the nascent defect distribution. A problem with such hybrid models is to obtain the proper temporal matching: since slow and stopped particles are present in simulated cascades almost from the beginning (Robinson 1990), it is not clear that the matching can always be achieved satisfactorily.

In view of the great advances in computing hardware mentioned above, a comment is in order concerning the relationships between MD codes and BCA codes. The former now follow collision cascades involving 10^4 to 10^6 atoms for simulated times up to a few picoseconds. Nevertheless, there will long be computations too massive for widespread study by MD, where swifter, but more approximate, computational methods are useful. Such applications include achieving precise statistics, where large numbers of cascades must be evaluated; cascade studies in complex materials, such as noncubic compounds, where it is difficult to determine equilibrium potentials reliably; and high-energy cascade studies. In addition, the fast response of BCA codes will remain useful for interpreting experimental data in surface physics studies and for rapid surveys of new topics. On the other hand, for cascade studies in highly symmetrical crystals containing atoms of very different masses, as, for example, Au-Cu alloys or UO_2, MD codes may be required to simulate accurately such processes as linear collision sequences along mixed atomic rows.

4 Interatomic Potentials

The interatomic potentials used in simulations of atomic collisions in solids may be divided into two groups. In close encounters, the change in potential energy is determined almost entirely by the positions of only two atoms, the other atoms of the target being merely spectators. In such encounters, a spherically-symmetrical, pairwise, repulsive interaction potential is appropriate, reflecting the essentially atomic nature of the distribution of electrons about the nuclei. Most BCA models use only these potentials although potentials with attractive parts are easily employed (Eckstein et al. 1992). At distances approaching or exceeding the normal separations of atoms in crystals, however, several atoms contribute significantly to changes in the potential energy. The electron distributions reflect the binding of the atoms in the target. Such binding effects may be supplied by the boundary conditions on a numerical crystallite, by spherically-symmetrical potentials with attractive regions, by many-body potentials, or by combinations of these. The two interaction ranges are considered separately.

4.1 Potentials for Close Encounters

Pairwise potentials for close encounters are often taken as the internuclear Coulomb repulsion, screened by a function describing the distribution of atomic electrons about the two nuclei. The very difficult problem of accurately evaluating the screening function must be approximated in various ways. First, dynamical effects on the electrons of the relative motion of the nuclei are neglected: this is the well-known Born-Oppenheimer approximation. Failure of this approximation in fast collisions probably cannot be distinguished from electron promotion and other inelastic effects discussed later. Second, the possible formation of molecular states from the atomic states of the colliding atoms must be considered. One important line of development assumes that the electron densities about the colliding atoms experience no redistribution, but may simply be superposed (Gombás 1956, Gordon & Kim 1972), with corrections to the kinetic energies of the electrons as well as corrections for electron exchange and correlation. These corrections are based on the properties of a uniform gas of free electrons of the same density. The atomic electron distributions may be taken from the Thomas-Fermi statistical model of the atom (Gombás 1956) or more accurate atomic wavefunctions may be used (Gordon & Kim 1972). When the two atoms approach each other slowly, however, there may be time for the electrons to form molecular states: see Dodson (1990, 1991) and Nakagawa (1990) for discussions of bonding effects in slow encounters. Instead of merely superposing the atomic electron distributions, so-called ab initio methods may be used to treat the molecular problem.

Molière (1947) proposed a numerically convenient approximation to a screening function derived from the Thomas-Fermi statistical model of the atom (Gombás 1956), which has the screening length

$$a_{\mathrm{TF}} = \left(\frac{9\pi^2}{128}\right)^{1/3} \frac{a_{\mathrm{H}}}{Z^{1/3}} \tag{1}$$

where Z is the atomic number of an atom and a_{H} is the Bohr radius (52.9 pm). Firsov (1957) and Lindhard et al. (1968) used the statistical model as a basis for developing approximate interatomic potentials. They expressed their results compactly by using the atomic Thomas-Fermi screening function with a screening length given by Eq. (1) with

$$\begin{aligned} \text{Firsov: } Z &= \left(Z_1^{1/2} + Z_2^{1/2}\right)^2 \\ \text{Lindhard: } Z &= \left(Z_1^{2/3} + Z_2^{2/3}\right)^{3/2} \end{aligned} \tag{2}$$

Ziegler et al. (1985) applied a local-density model which uses atomic electron distributions based on self-consistent Hartree-Fock atomic wavefunctions and includes free-electron corrections to the electron kinetic energy and for exchange and correlation (Gordon & Kim 1972; see Gombás 1956 and Ziegler et al. 1985 for additional references) to determine interatomic potentials. The resulting potentials should describe rather accurately the interactions of isolated pairs of atoms in their ground states. Ziegler et al. (1985) used the potentials computed for a large number of atom pairs as the basis for fitting a 'universal' (ZBL) potential for which they propose a screening length given by Eq. (1) with

$$\text{ZBL: } Z = \left(Z_1^{0.23} + Z_2^{0.23}\right)^3$$

The dependence of this screening length on the Z_i is weaker than those in Eq. (2). The need for a weaker dependence had already been noted (Robinson 1981, Eckstein 1991) and, in fact, the Molière potential is often used with screening lengths other than those in Eq. (2). The ZBL and Molière screening functions are both sums of exponentials:

$$\begin{aligned} V(r) &= \frac{Z_1 Z_2 e^2}{r} \phi\left(\frac{r}{a}\right) \\ f(x) &= \sum_{j=1}^{m} \alpha_j \; e^{-\beta_j x} \end{aligned}$$

$$\begin{aligned} \text{Moliere}: m &= 3; \\ \alpha &= \{0.35, 0.55, 0.10\}; \\ \beta &= \{0.3, 1.2, 6.0\} \\ \text{ZBL}: m &= 4; \\ \alpha &= \{0.02817, 0.28018, 0.50986, 0.18179\} \\ \beta &= \{0.2016, 0.4029, 0.9423, 3.2\} \; . \end{aligned}$$

These potentials are 'universal' in the sense that no explicit Z-dependence remains in the screening function. The ZBL potential is used to establish the approximate treatment of atomic scattering used in the TRIM codes (Biersack 1987) and is available in MARLOWE (Robinson 1992a). It is also used as the core portion of the interatomic potential in several MD codes (Valkealahti & Nieminen 1987, Diaz de la Rubia & Guinan 1990, Chou & Ghoniem 1991).

The ZBL potential is a reasonable description of the interactions of isolated pairs of atoms, especially those from the first half of the periodic table, as long

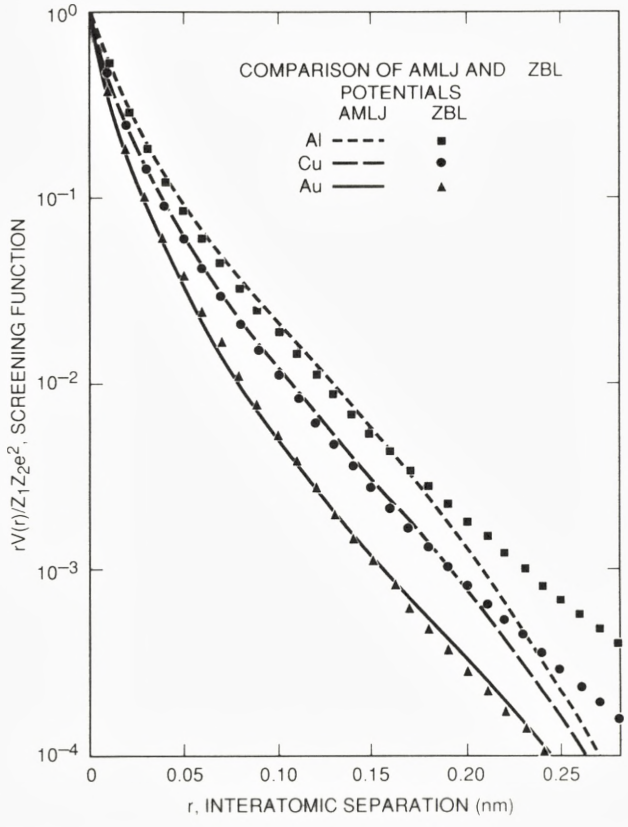

Figure 2. A comparison of the AMLJ (Nakagawa & Yamamura 1988, Nakagawa 1991) and ZBL (Ziegler et al. 1985) screening functions for Al, Cu, and Au atom pairs. The nearest-neighbor distances in the three crystals are 0.286, 0.256, and 0.288 nm, respectively.

as they remain in their ground-states (and as long as binding effects can be ignored). For heavier atoms, relativistic corrections should be included in the atomic wavefunctions, using, for example, the method of Tucker et al. (1969); tables of wavefunctions and electron densities are available for all atoms (Carlson et al. 1970, Lu et al. 1971).

Nakagawa & Yamamura (1988) used the relativistic electron densities of Carlson et al. (1970) in a statistical local-density calculation of the interactions of many pairs of atoms similar to the work of Ziegler et al. (1985). The atoms were confined to Wigner-Seitz cells representing the densities of the appropriate solids. An average modified Lenz-Jensen (AMLJ) potential was used to summarize the

results. The screening function is

$$\phi(r) = e^{-\alpha_1 r + \alpha_2 r^{3/2} - \alpha_3 r^2}$$

with (Nakagawa 1991):

$$\begin{aligned}
\alpha_1 &= \frac{1.706}{a_{\mathrm{H}}} \left(Z_1^{0.307} + Z_2^{0.307} \right)^{2/3} \\
\alpha_2 &= \frac{0.916}{a_{\mathrm{H}}^{3/2}} \left(Z_1^{0.169} + Z_2^{0.169} \right) \\
\alpha_3 &= \frac{0.244}{a_{\mathrm{H}}^{2}} \left(Z_1^{0.0418} + Z_2^{0.0418} \right)^{4/3}
\end{aligned}$$

[Note that the original paper (Nakagawa 1991) uses atomic units and thus omits a_H from these formulas.] The AMLJ screening function is not 'universal': the three parameters show different Z-dependences so that the shape of the function varies with the atoms involved in the encounter. This behavior reflects the differing importance of the components of the total energy for different atom pairs, especially the density corrections to the electron kinetic energy and the exchange energy. The two screening functions are compared in Fig. 2 for Al, Cu, and Au atom pairs. They agree well for small separations, but significant differences appear at separations approaching the nearest-neighbor distances, especially in the lighter elements. These differences probably originate mainly in electron kinetic energy corrections resulting from confinement of the atoms in Wigner-Seitz cells. Evidently, relativistic corrections are small. The AMLJ potential is more efficient computationally than the ZBL: preliminary MARLOWE calculations (Robinson 1992c) required about 20% less time with the AMLJ potential than with the ZBL.

Several attempts have been made to establish interatomic potentials on a more fundamental basis. SCF methods were used to study potentials for Al-H (Sabelli et al. 1978) and Al-Al (Sabelli et al. 1979) interactions. In both cases, the changing symmetry of the ground-state with separation was followed, giving a clear picture of the effects of electron promotion on the potential. In the Al-Al potential, a 'kink' appears in the screening function near $2a_H$. For larger separations, the SCF potential is in excellent agreement with the local-density potential of Wilson et al. (1977).

Ab initio methods were used to evaluate potentials for a number of pairs of atoms for use in sputtering calculations. A potential was obtained for the interaction of Ar^+ with Cu, at separations from about 40 to about 140 pm, using the $^1\Sigma^+$ state of $CuAr^+$ as the basis (Broomfield et al. 1988). Figure 3 compares a screening function derived from this work with those for the ZBL potential and a Molière

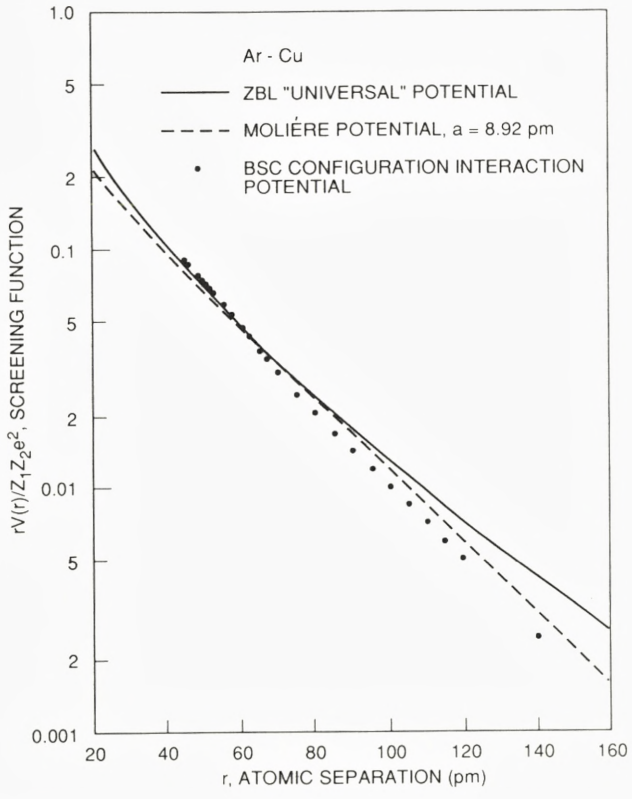

Figure 3. Screening functions for Ar-Cu collisions. The configuration-interaction potential of Broomfield et al. (1988) is compared to the ZBL 'universal' potential (Ziegler et al. 1985) and to a Molière potential with the screening length 8.92 pm (Hou & Robinson 1979).

potential with a screening length used in earlier sputtering calculations (Hou & Robinson 1979; Shulga 1982 made a similar choice). As the figure shows, the three potentials agree closely with one another. This result supports the use of the ZBL potential, but also makes it clear that the strategy of using the screening length as a fitting parameter in the Molière potential has merit. Similar potentials were calculated for Ar^+-Si and Si-Si (Stansfield et al. 1989) and for Cu-Si and Cu-Cl (Broomfield et al. 1990). Similar consistency was found between these potentials and the ZBL. In the Ar-Cu system, an avoided level crossing was noted at about 40 pm (that is, at about 1.8 keV), within which the model became unphysical and other level crossings were also mentioned. Similar crossings were found in the Ar-Si

and Si-Si systems also. Such crossings signal that changes in the ground-state of the system must be expected and that electrons are likely to be promoted to excited states during an encounter (Fano & Lichten 1965, Lichten 1967, 1980, Barat & Lichten 1972).

Keinonen et al. (1991) reported potentials for K-Cl, Na-Cl, and Cl-Cl interactions, calculated for atomic clusters using density-functional theory. Their potentials also agree reasonably well with the ZBL ones.

Hsieh et al. (1992) used LCAO-MO calculations on small clusters to test a hybrid many-body potential with a Molière core. They obtained reasonable agreement for Cu-Cu and Ni-Ni interactions at energies up to 100 eV or so, but above this, their potential was more strongly repulsive than the Molière. It is not clear to what extent this results from many-body effects on the interaction between the closely-separated atoms, nor what changes would occur if the cluster were allowed to relax.

O'Connor & Biersack (1986) compared the ZBL, Molière, and other potentials with a large number of empirical potentials and found the ZBL to be the most suitable, although some of the others are sometimes useful. Other comparisons, with generally similar results were made by Chang et al. (1986, 1987) and by Chini & Ghose (1989). When a uniform beam of swift atoms is scattered from a target atom by a repulsive interaction, there is a conical region behind the target into which the beam atoms cannot penetrate. The size of this so-called shadowcone can be measured experimentally (see Eckstein 1991, p. 22, and Aono 1984). Chini and Ghose (1989) cite the Born-Mayer potentials of Andersen & Sigmund (1965) as giving good agreement with experimental shadowcones. Kato et al. (1988) find the ZBL potential to give a better account than does the Molière for experimental shadowcones observed in the scattering of 1 keV rare gas ions from a TaC (001) surface, especially when suitable account is taken of the effects of the image potential in accelerating the incident particle. The inclusion of image-potential effects might alter the other comparisons also. The AMLJ potential was compared (Nakagawa & Yamamura 1988, Nakagawa 1991) with experimental range data in Si using the ACAT code (Takeuchi and Yamamura 1983). The agreement was as good or better than O'Connor and Biersack (1986) found for the ZBL potential. Eckstein et al. (1992) compared range, sputtering, and ion reflection data, calculated for several two-body potentials with a version of the BCA code TRIM.SP (Biersack & Eckstein 1984), modified to integrate the two-body equations of motion instead of using the usual TRIM scattering approximations. The potentials were the Molière with the Firsov screening length, the ZBL, the so-called KrC potential (Wilson et al. 1977) with the Firsov screening length, and an ab initio Si-Si potential with an attractive region (Heinemann et al. 1990, Hackel et al. 1990; see also Eckstein 1991). Calculations were made for 0.1 to 10 keV Si on amorphous Si targets. Sputtering yields

and reflection coefficients with the three repulsive potentials differed from those for the ab initio potential for ions incident at near grazing angles where large impact parameters are important. Otherwise, good agreement was found among the four potentials. These results support the otherwise universal use of purely repulsive potentials in BCA calculations.

The local-density method used in the ZBL and AMLJ calculations is restricted to atoms in their electronic ground-states, as were the other calculations cited. There is ample evidence (Kessel & Everhart 1966, Garcia et al. 1973, Grizzi & Baragiola 1987, Yu 1991) of inelasticity in atomic collisions in the gas phase, as well as in sputtering. Excited atoms emerging from such encounters have altered electron-density distributions and will interact according to an altered, usually more repulsive, potential-energy function in later collisions. Such effects are most important for the primary particle: since calculated sputtering yields are especially sensitive to the potential describing the interactions between the incident ions and the lattice atoms (Harrison 1981a, 1983, 1988, Broomfield et al. 1988), inelastic effects on this potential are likely to be significant. This sensitivity is explained by the result from analytical theory (Sigmund 1981) that sputtering yields closely follow the elastic stopping cross section of the incident particles. It is unlikely that the corresponding effects on interactions among the target atoms are important, as the great majority of them interact only at quite low energies, where inelastic effects will not greatly alter the electron-density distributions.

4.2 Many-Body Potentials

At the time of Andersen's (1987) review, almost all MD calculations in the atomic collisions field had been performed with pair potentials and models of this type are still used. One set of models uses a repulsive potential of the Born-Mayer type with crystal (meta)stability supplied by truncating the potential or by using boundary constraints (Averback et al. 1988, 1991, Caro et al. 1990, Diaz de la Rubia et al. 1987, 1989, Pan 1992, Pan & Sigmund 1990, Shulga & Sigmund 1990, 1991, Shulga 1991). In another set of models, the potentials are typically Morse potentials, splined to a suitable repulsive potential for close approaches between the atoms (Antonov et al. 1990, Averback et al. 1988, Betz et al. 1991, Broomfield et al. 1988, 1990, Diaz de la Rubia et al. 1989, Diaz de la Rubia & Guinan 1990, Harrison et al. 1987, Lo et al. 1987, Mazzone 1988, Pelletier et al. 1992, Shapiro et al. 1988, Shapiro & Fine 1989, Shapiro & Tombrello 1987, 1990a,b, 1991a,b, 1992a,b, Smith & Harrison 1989). Harrison (1983, 1988) discusses the use of Morse potentials.

For some purposes, pair-potential models are satisfactory and they are, moreover, more efficient computationally than more elaborate potentials. There are, however, many drawbacks (Finnis & Sinclair 1984, Carlsson 1990). First, purely

repulsive models lead inevitably to close-packed structures and so are restricted to fcc metals. Second, in all pair-potential models, the proper relationships of the elastic constants can be achieved only through boundary conditions on the numerical crystallite. Such measures allow calculations for bcc metals, but are not altogether satisfactory, especially if the target has a free surface. Moreover, pair-potential models are not able to give a good account of selvage effects (relaxations, reconstructions), potentially important in sputtering, or of other defect properties, important in cascade studies as well as in more general solid-state contexts. Consequently, many-body potentials have been developed to better represent the properties of solids.

Two main classes of many-body potentials have been developed for use in studies of transition metals and semiconductors. The theory underlying these potentials and the relationships between them are reviewed in detail by Carlsson (1990). The basic idea is to express the configurational energy of a solid as the sum of two terms:

$$E_C = \frac{1}{2}\sum_{i \neq j} V_2(\mathbf{R}_i, \mathbf{R}_j) + \sum_i U\left[\sum_j g_2(\mathbf{R}_i, \mathbf{R}_j)\right]$$

where the $\mathbf{R}_i$ are the positions of the atoms, V_2 is a pair potential, g_2 is a pair function describing the local environment of atom i in terms of the positions of its neighbors, and U is a function describing how the energy of atom i depends on its environment. It is possible to go further and allow U to depend on three- or more-body environmental terms, thus introducing angular forces into the picture, and this is generally required for substances with strongly-directional covalent bonds or for certain problems involving differences between similar structures. The pair potential is often taken as an exponential (Born-Mayer) repulsion, but any of the potentials discussed above could be employed. Furthermore, there is some arbitrariness in the division of E_C between V_2 and U: any term in U that is linear in the appropriate environmental parameter (see below) can be described by a pair potential.

One class of many-body potential is based on a tight-binding (TB) analysis (Cyrot-Lackmann 1968, Ducastelle 1970). When a solid is formed, the partly-filled atomic valence orbitals broaden into bands: this broadening supplies the attractive part of the bonding energy. It is assumed further that the valence-band electronic density of states on a particular site can be given in terms of radial contributions from the neighboring atoms. The binding function U is then expressed in terms of the moments of the density of states. Since the first moment vanishes (Carlsson 1990), the simplest approximation limits the model to the second moment, which becomes the environmental parameter, describing the width of the band, but ignoring its detailed shape. By adding higher moments to a TB model,

various angular terms can be included in the interaction potential.

Another class of many-body potential is based on the so-called embedded-atom method (EAM) (Daw & Baskes 1984, Foiles et al. 1986). The solid is regarded as being assembled one atom at a time: the bonding energy is the energy gained by embedding one atom in the background electron density of all the other atoms. This density is the environmental parameter in the EAM. To make the treatment tractable for simulations, it is assumed that the bonding energy associated with a particular atom is determined by the local background electron density at the site of the embedded atom and it is further assumed that this density can be constructed as a superposition of radial functions centered on the other atoms. Angular terms can be added to EAM potentials by including gradients and higher derivatives of the electron density. It should be mentioned that the substantial formal similarities between the EAM and TB approaches (Carlsson 1990) often makes a distinction between them unnecessary or even impossible (see, for example, Johnson 1991).

Much like the EAM is so-called effective-medium theory (Jacobsen et al. 1987), useful in modelling various bulk and surface properties of metals. Each atom is embedded in a uniform electron density provided by its neighbors. The neighbor densities are averaged over the region occupied by the embedded atom. The parameters of the potential are then evaluated in the local-density approximation. Effective-medium potentials have not been used so far in atomic-collision calculations. See Carlsson (1990) for comparisons of the EAM and effective-medium theory.

Both the TB and EAM potentials may be parameterized and the parameters fit to such experimental data as the lattice constant, the cohesive energy, the bulk modulus, the elastic constants, the vacancy-formation energy, properties of the diatomic molecule, and surface properties. It is not possible to fit all experimental data with great precision and compromises are usually necessary, tailored to the needs of the particular simulation. Furthermore, fitting the parameters of many-body potentials to elastic-constant data in crystals without inversion symmetry poses special problems because of the effects of inhomogeneous strains (van Midden & Sasse 1992).

The EAM was originally applied to fcc metals, but Johnson & Oh (1989) and Adams & Foiles (1990) have described EAM models suitable for bcc metals. Suitable EAM potentials cannot be found for most of the hexagonal metals (Pasianot & Savino 1992), but TB potentials of the Finnis & Sinclair (1984) type are available (Igarashi et al. 1991), although these have been criticized (van Midden & Sasse 1992). A modified EAM was described recently by Baskes (1992).

Typical recent examples of EAM potentials are given by Garrison et al. (1988), Chen et al. (1990), and Guellil & Adams (1992). Recent TB potentials are given by Igarashi et al. (1991), Loisel et al. (1991), and Gades & Urbassek (1992). Like

the pair potentials, both EAM and TB potentials may be combined with one of the repulsive potentials discussed above. Hsieh et al. (1992) use a cubic spline to connect a Molière core to the two-body part of an EAM potential; over the same range of separation, they smoothly remove the many-body part.

The EAM was used for simulations of low-energy hydrogen-atom reflection from metals by Baskes (1984), but was used first in sputtering simulations by Garrison and her coworkers (Garrison et al. 1988, Lo et al. 1988, Wucher et al. 1992, Wucher & Garrison 1992a,b, 1993). It is used in simulations of displacement cascade development (Diaz de la Rubia & Guinan 1990, 1991; Chou & Ghoniem 1991; Proennecke et al. 1991) and in studies of cluster impacts (Hsieh et al. 1992), as well as in other sputtering simulations (Gades & Urbassek 1992, Karetta & Urbassek 1992). Diaz de la Rubia & Guinan (1990) also use TB potentials of the type developed for bcc metals by Finnis & Sinclair (1984).

Angular forces are required to stabilize structures with strongly-directed chemical bonds, such as the diamond-structure semiconductors. A tight-binding analysis (Carlsson 1990) can be used to show how the inclusion of third- and fourth-moments in the evaluation of the bonding energy leads to terms depending on the positions of three or four atoms and thus introduces forces depending on the angles between the bonds. However, most simulation work uses not only empirically-fitted parameters, but also empirical dependences on bond angles.

A potential proposed by Stillinger & Weber (1985) combines two- and three-body terms. The former is a generalized Morse potential; the three-body term involves the lengths of three interatomic vectors and the angles between them. It was used in sputtering simulations by Stansfield et al. (1989). Tersoff (1986, 1988a,b,c) has proposed alternative potentials, also using a generalized Morse potential, but here the parameters are made functions of the local environment, including bond lengths and angles. The hazards in such empirical potentials are illustrated by Tersoff's first potential for Si (Tersoff 1986), which proved not to have the diamond lattice as its ground state (Dodson 1987a), a problem later corrected (Tersoff 1988a). Several alternative Si potentials have been proposed (Brenner & Garrison 1986, Baskes 1987, Dodson 1987a, Biswas & Hamann 1987). Similar potentials have been developed for C (Tersoff 1988b, Brenner 1990) and GaAs (Smith 1992). Several simulations of sputtering and related topics have used such potentials (Dodson 1987b,c, 1990, Dodson & Taylor 1987, Smith et al. 1989, 1990, Mowrey et al. 1991, Smith & Webb 1991, 1993). Several studies, summarized by Carlsson (1990), examined reconstructions of Si surfaces using the potentials cited, with mixed success. One must express some concern, therefore, that the assumed angular dependences are not accurate near surfaces and may be unsatisfactory for sputtering simulations in some cases.

An empirical potential has been proposed for MD calculations in the high-

temperature perovskite superconductor $YBa_2Cu_3O_{7-\delta}$ (Chaplot 1988, 1989, 1990). This potential was used for low-energy radiation-damage studies (Cui et al. 1992). Kirsanov & Musin (1991) reported some low-energy radiation-damage calculations in this material using a Morse-type pair-potential with boundary constraints. Mention must also be made of potentials for use with alkali halides (Catlow et al. 1977) and for the interactions of rare-gas atoms with alkali halide ions (Ahlrichs et al. 1988). These potentials may be described as combining Born-Mayer repulsive interactions with attractive terms of the van der Waals power-law type. They have been used in recent studies of cluster impacts (Cleveland & Landman 1992).

5 Inelastic Energy Losses

Besides losing energy in scattering from the atoms of the target, energetic particles also lose energy by exciting electrons, both those of the medium and those of the particles themselves. Stoneham (1990) has reviewed the effects of ion-electron energy exchanges on collision-cascade development in a general way. In metals and semiconductors, the inelastic energy loss is calculated from the dynamic response of a uniform electron gas to the passage of a charged particle, a topic reviewed by Echenique et al. (1990). The theory accounts very well for the stopping of protons in matter over a wide range of kinetic energy, from a few keV to many MeV. The effective-charge theory of Brandt & Kitagawa (1982) allows this treatment to be extended to other particles. At low projectile kinetic energies, however, experimental data do not exist for testing a theory of electronic stopping and the situation is ambiguous. Finally, at the very lowest energies allowance must be made for the ordinary electron-phonon interaction, the importance of which was emphasized by Flynn and Averback (1988).

At several points in the following discussion, the inelastic energy losses are related, either explicitly or by implication, to the local density of electrons in the stopping medium. There are two problems with this formulation. First, such losses involve the excitation of target electrons that are not local to the track of the projectile: one would expect to integrate the excitations over the target electron density in a region surrounding the projectile track, with a weighting function to describe the losses as a function of the distance to the electrons in question. Second, the inelastic energy losses involve excitations of the projectile electrons themselves: again an integral over the excitations is required, this time using the electron-density distribution in the projectile. Thus, significant reservations must be expressed about formulations that do not include such integrations, but restrict themselves to the local density (see Sigmund 1991, Mikkelsen et al. 1992).

5.1 Inelastic Energy Losses in BCA Models

Some BCA simulation models treat inelastic energy losses as depending on the energy of a projectile and on the pathlength it traverses, but not on the particular surroundings of the trajectory segment. There are, therefore, no correlations between the elastic and the inelastic energy losses. Such models may be said to use 'nonlocal' inelastic losses, since no properties local to the particular path segment enter the calculation. At low energies, the nonlocal electronic stopping cross section usually takes the form (Fermi & Teller 1947, Lindhard & Scharff 1961)

$$S_e(E) = kE^{1/2} \tag{3}$$

where E is the projectile kinetic energy and the parameter k is derived from experiment, from the well-known LSS theory (Lindhard & Scharff 1961, Lindhard et al. 1968), or otherwise. This form is included as an option in both MARLOWE (Robinson 1989) and TRIM.SP (Biersack 1987). It may be used alone or mixed in some proportion with local inelastic energy losses. In at least one case (Cowern & Biersack 1983), a version of TRIM included electronic energy-loss straggling using an approximate treatment by Bohr (1915).

An alternative formulation of the inelastic stopping problem follows Firsov (1959) in making the energy lost inelastically in a collision depend on how closely two atoms approach one another, providing a strong correlation between the elastic and the inelastic energy losses in individual encounters. Firsov assumed the relative energy in the collision to be high enough that the projectile was undeflected and used an asymptotic form of the Thomas-Fermi screening function (Gombás 1956), obtaining for the inelastic loss in a single collision

$$Q(p, E) = \frac{\alpha E^{1/2}}{(1 + \beta p)^5}$$

where p is the impact parameter and α and β are numerical parameters.

Firsov's formula may be corrected approximately for scattering by replacing p with $R(p, E)$, the apsis in a collision (Robinson & Torrens 1974). The asymptotic Thomas-Fermi screening function may be replaced by an exponential function, which has a more realistic behavior at large distances (Oen & Robinson 1976). The result may be written

$$Q(p, E) = kE^{1/2} \frac{\gamma^2}{2\pi a^2} e^{-\gamma R(p,E)/a} \tag{4}$$

where a is a screening length and γ is a parameter, taken originally as 0.3 to connect Eq. (4) with the Molière potential. Under the conditions of the impulse approximation, this formulation gives the stopping cross section of Eq. (3), which

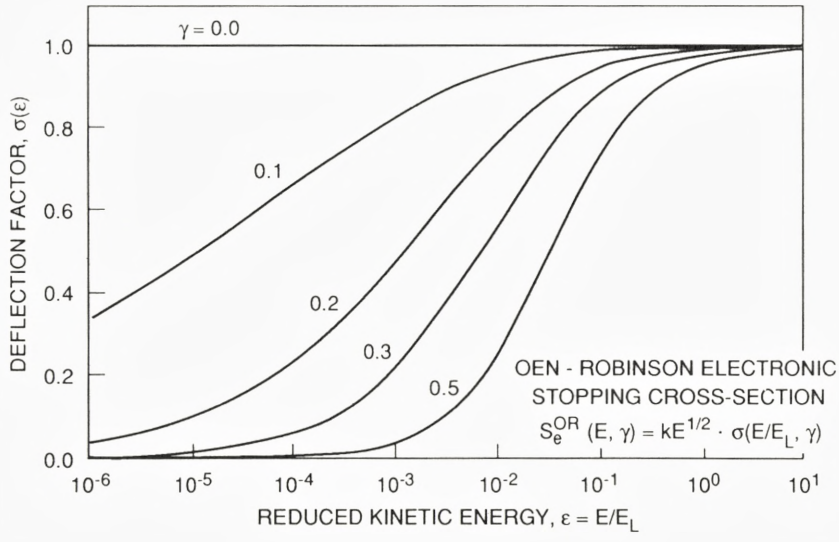

Figure 4. The deflection factor in the OR electronic stopping cross section model, evaluated for the Molière potential (Robinson 1992c). The original OR work (Oen & Robinson 1976) used $\gamma = 0.3$.

is proportional to the projectile velocity, but for lower energies, it falls more rapidly than implied by Eq. (3). The OR stopping cross section is

$$S_e^{\mathrm{OR}}(E) = 2\pi \int_0^\infty pQ(p,E)dp = kE^{1/2}\sigma(\epsilon)$$

The deflection factor is

$$\sigma(\epsilon) = \int_0^\infty ue^{-(\gamma/a)R(au/\gamma,\epsilon)}du,$$

where $\epsilon = E/E_{\mathrm{L}}$ is the usual reduced energy and

$$E_{\mathrm{L}} = \frac{Z_1 Z_2 e^2}{a}\frac{m_1+m_2}{m_2},$$

with $Z_1 e$ and $Z_2 e$ the nuclear charges of the projectile and target atoms, respectively, and m_1 and m_2 their masses. Figure 4 shows $\sigma(\epsilon)$ for the Molière potential, with several values of γ. The OR model cuts off the electronic energy losses at low projectile velocities in a plausible manner. The original connection between the OR model and the Molière potential is not essential: any potential can supply a

and $R(p, E)$, k can be determined as in the nonlocal model, and γ can be used as a free parameter with the nominal function of making the inelastic energy loss follow the electron density in the target atom. Lennard et al. (1992) used the OR model with modified constants to fit the stopping of low-velocity ^{27}Al ions in carbon. The effects on electronic stopping of the impact parameter cutoff used in BCA codes is discussed elsewhere (Oen & Robinson 1976, Robinson 1993).

Another method of treating inelastic energy losses in a local manner is to relate the stopping cross section to the local electron density at the position of a projectile. Two models of this kind were designed specifically for low-energy ion implantation in Si. Azziz et al. (1985, 1987) used linear response theory (Echenique et al. 1990) to calculate the energy transferred to an electron, viewed as an oscillator, as a function of impact parameter. A method outlined by Ferrell & Ritchie (1977) was used to average the loss over the electron distributions of the two colliding particles. The final loss calculated for B-Si collisions as a function of impact parameter was said to agree well with both the Firsov and OR models and the energy dependence of the inelastic stopping cross section was similar to the LSS function. Klein et al. (1990) used the proton stopping cross section of Echenique et al. (1981) and the effective-charge theory of Brandt & Kitagawa (1982), but used a local electron density for Si based on a muffin-tin approximation. Both Azziz et al. (1985, 1987) and Klein et al. (1990) modified MARLOWE to use their stopping cross section formalisms and both claim improved agreement between simulation and experiment for B implantation distributions in Si. Some doubt must be expressed about the validity of response functions derived for the uniform electron gas for modeling the response of the very nonuniform electron distributions in atoms.

Kaneko (1990a,b) developed a wave-packet theory for inelastic energy losses which shows losses that decrease with impact parameter less rapidly than they do in the OR model when applied to Pb. However, changes in the screening length and proper accounting for deflections would alter the comparisons. Unlike most other workers, Kaneko also discussed the impact parameter dependence of the straggling of the electronic energy loss. Inclusion of straggling is important in comparing simulations with experiment, especially at higher energies.

Murthy & Srinivasan (1993) used a different scheme to study the implantation of 7 MeV He^{++} in Si under channeling conditions. They modified MARLOWE to use the nonlocal electronic energy-loss formulation of Burenkov et al. (1980), coupled with a function describing the electron density in various important channels in Si. See Logan et al. (1992) for details.

5.2 Inelastic Energy Losses in MD Models

Nonlocal inelastic energy losses can be included in MD models by adding to the equations of motion a frictional term based on Eq. (3):

$$M\ddot{\mathbf{x}} = \mathbf{F} - \beta\dot{\mathbf{x}} \tag{5}$$

where M is the mass of an atom, $\mathbf{F}$ represents the conservative forces, $\beta = nk(M/2)^{1/2}$, and n is the target density. The frictional force represented by Eqs. (3, 5) is directed along the instantaneous trajectory of the projectile. The relaxation time for inelastic energy losses, M/β, is ~ 0.5 ps for typical cases, assuming the LSS theory for k. Only a few programs (Valkealahti & Nieminen 1987, Jakas & Harrison 1984, Harrison & Jakas 1986b) include nonlocal inelastic energy losses, mainly on the ground that they are insignificant at low initial kinetic energies.

Caro & Victoria (CV) (1989) describe an MD model for metals which includes local electronic effects. They identify two regimes: at relatively high kinetic energies, there are inelastic energy losses described by Eq. (5) with β depending on the local electron density in the spirit of the OR model; at low energies, there are interactions between slowly moving atoms ('phonons') and conduction electrons which equilibrate the excess kinetic energy of the atoms with the electrons and permit the ordinary metallic heat conductivity to carry the energy away from the cascade region (see Flynn & Averback 1988). To model the electron-phonon interaction, they turn to Langevin's equation of motion, well-known in the theory of Brownian motion and other areas of statistical physics (Chandrasekhar 1943, Uhlenbeck & Ornstein 1930, Wang & Uhlenbeck 1945; see Wax 1954). This takes the form

$$M\ddot{\mathbf{x}} = \mathbf{F} + \boldsymbol{\eta}(t) - \beta\dot{\mathbf{x}} \tag{6}$$

where $\boldsymbol{\eta}(t)$ is a random force and β now measures the strength of the coupling of the atomic system to the heat bath represented by the electrons. Each component of $\boldsymbol{\eta}(t)$ obeys a Gaussian distribution with mean value zero and variance $2\beta k_{\mathrm{B}}T$, where k_{B} is Boltzmann's constant and T is the temperature of the reservoir. In the regime where Eq. (6) applies, M/β is the relaxation time for electronic heat conduction, ~ 10 ps. Equations (5) and (6) are similar, but the frictional coupling parameters differ by more than an order of magnitude.

CV unify the treatment of the two regimes empirically by setting

$$\beta = A\ \ln[\alpha\rho^{1/3} + b] \tag{7}$$

where ρ is the local electron density, A and b are fitting parameters, and

$$\alpha = (3\pi^2)^{1/3}\ a_{\mathrm{H}} = 3.0937\ a_{\mathrm{H}}\ .$$

The value of A is near $(h/3)(Z/\pi a_{\mathrm{H}})^2 = 8 \times 10^{-12} Z^2$ g/s. The electron density in Eq. (7) is derived from the many-body interaction potential used for the conservative forces, such as an EAM potential with allowance made for the repulsive potential at small interatomic separations.

The CV model provides an empirical treatment of electronic effects in cascade simulations in much the same spirit that the empirical many-body potentials do for the conservative forces. The model is used in the MOLDYCASK code (Diaz de la Rubia & Guinan 1990, 1991, Proennecke et al. 1991), but has not been applied to sputtering studies. Since the time scale for electron-phonon interactions is generally much greater than that for sputtering, it is likely that a CV model including only the local electron density dependence of the electronic stopping cross section would suffice for most sputtering simulations, subject always to the caveat expressed above about the use of local densities for this purpose.

5.3 The Effects of Inelastic Energy Losses in Sputtering

As Andersen (1987) pointed out, it has long been realized that the LSS model (Lindhard et al. 1963, 1968) implies substantial losses of energy to electronic excitations, even at very low kinetic energies. The role of these low-energy inelastic losses in displacement damage was discussed by Robinson & Oen (1982). They pointed out that the so-called modified Kinchin-Pease (or NRT) model (Norgett et al. 1975) incorrectly discounts electronic energy losses occurring below the cascade multiplication threshold in calculating the damage energy. An approximate correction can be made by defining $L = 2E_d/\kappa$, where E_d is the displacement threshold and κ is the displacement efficiency, and then writing the mean number of defects as

$$< \nu > = \frac{\hat{E}(E)}{\hat{E}(L)}, \qquad L \leq E \leq \infty$$

where $\hat{E}(E)$ is the conventional damage energy from the LSS treatment. The correction factor $L/\hat{E}(L)$ can increase the estimated damage by 20% or more.

Several claims were made during the past decade that inelastic energy losses play a major role in determining sputtering yields. This conclusion was reached on the basis of BC (Robinson 1983), MC (Harrison 1988, Jakas & Harrison 1984, Harrison & Jakas 1986b, Biersack & Eckstein 1984, Eckstein & Biersack 1984), and MD (Harrison 1988, Jakas & Harrison 1984, Harrison & Jakas 1986b) simulations as well as on a numerical transport-theory calculation (Jakas & Harrison 1985), so appears quite general. It was based, however, on simulations with nonlocal electronic stopping and, in at least one case (Robinson 1983), an artifact in the simulation was partially responsible.

Table 2: The Effect of 'Last Flight' Electronic Energy Losses on Self-Sputtering Yields in Polycrystalline $\alpha - U$ (Robinson 1983, 1992c).

Incident Energy E (keV)	Sputtering Yield (atoms/ion) Local Energy Losses	Nonlocal Electronic Energy Losses 'Last Flight'	Nonlocal Electronic Energy Losses No 'Last Flight'	Final Path $\langle z \rangle$(nm)
0.5	1.703±0.018	0.703±0.011	1.037±0.014	0.378
1	3.324±0.039	1.591±0.025	2.157±0.029	0.290
3	7.463±0.123	3.657±0.054	4.872±0.091	0.272
5	10.600±0.190	5.203±0.111	6.757±0.129	0.247
kn = 2.625 $eV^{1/2}$/nm		U_s= 5.37 eV	p_c = 0.240 nm	

A large difference was found in the self-sputtering yields of polycrystalline α-U calculated with nonlocal and local loss models, using MARLOWE Version 11.7 (Robinson 1983): nonlocal losses were evaluated even for trajectory segments which did not end in a collision, but extended beyond the reach of the potential at the target surface. In contrast, local losses were evaluated only for trajectory segments ending in collisions. It can be shown that, when the planar model (Robinson 1981, Hofer 1991) is used to describe surface binding, the inclusion of 'last flight' inelastic energy losses is equivalent to increasing the surface binding energy U_s. The effective surface binding energy is

$$U_{\text{eff}} = U_s \left(1 + \frac{kn \langle z \rangle}{2U_s^{1/2}} \right)^2 \tag{8}$$

The electronic stopping cross section is $kE^{1/2}$, n is the target density, and $\langle z \rangle$ is the average length of the last flight segment. The effects of such 'last flight' losses are shown in Table 2, which compares yields calculated with local inelastic energy losses, with nonlocal losses calculated as in MARLOWE Version 11.7, and with nonlocal losses calculated as in MARLOWE Versions 12 and 13, where they are omitted on 'last flights'. The table also shows the mean path deduced from the two nonlocal-loss calculations using Eq. (8). As expected, $\langle z \rangle$ is somewhat greater than p_c, the impact parameter cutoff, which determines how far an atom must move away from the crystal surface plane before it no longer interacts with target atoms.

Table 2 shows how sensitive simulations can be to seemingly unimportant details. The difference between the local- and nonlocal-loss models is much greater for U than for lighter elements: here ϵ ranges from $\sim 10^{-6}$ to $\sim 10^{-3}$, so that the stopping cross section in the local model is never more than 20% of the nonlocal value. Even so, about one-third of the difference is accounted for by the 'last flight' effect. For the sputtering of Ni by Ne (Eckstein & Biersack 1984), the difference

between the two models is less, but the role of 'last flights' is even greater. Both MARLOWE and TRIM.SP were modified some years ago to eliminate the 'last flight' effect.

At the present time, it is not possible to establish unambiguously whether or not low energy particle interactions in solids are dominated by electronic energy losses as implied by some of the simulations cited above. It is clear that if such losses continue to the lowest energies, as implied by the LSS theory, they must eventually be dominant (see Jakas & Harrison 1985). If the electronic stopping process is to go over into the ordinary electron-phonon interaction at thermal energies, however, the cross section must finally be an order of magnitude lower than the LSS value: see the discussion of the CV model above. What is needed is a detailed theoretical analysis of the transition between the electronic-stopping regime and the electron-phonon regime. This remains one of the most difficult and obscure problems in particle-solid interaction theory at the present time.

6 Surface Modelling

The surface of an irradiated target has a decisive influence on the number of particles sputtered and on their distributions in direction and kinetic energy. This is clear from experiments (Hofer 1991), especially those on single crystal targets, which show characteristic angular distributions. The surface is also responsible for transforming the energy distribution of atoms recoiling inside the target, more-or-less proportional to E^{-2}, into one characteristic of sputtered atoms, with a maximum near half the surface binding energy (Sigmund 1981, Thompson 1968). Thus, some attention must be given to modelling the target surface in a realistic manner. There are four issues to resolve: the magnitude and detailed nature of the surface binding, the fate of atoms which fail to surmount the binding barrier, target selvage effects, and the effects of prolonged irradiation. Surface binding is inherent in stable MD models, especially those with realistic many-body potentials, but must be considered carefully in BCA models; there are problems also in MD models using only pair potentials, since these are known (Robinson 1981) not to deal correctly with the target selvage. Geometrical changes in selvages include relaxations of near-surface atoms away from their ideal crystal positions and, even more drastically, reconstruction of the crystal surface. Relaxation effects and reconstruction of some metal surfaces have been studied with EAM models (Foiles et al. 1986, Chen et al. 1986, Foiles 1987) and the reconstruction of one Si surface has been accounted for with many-body potentials (Abraham & Batra 1985, Khor & Das Sarma 1987). There are also undoubtedly selvage effects on interaction potentials, inelastic energy losses, and surface binding energies. Nevertheless, such selvage

effects are generally ignored in sputtering simulations, on the ground of their likely low significance (Harrison 1988). While caution in this area is suggested, the large uncertainties in other areas make the position tenable for the present.

6.1 Surface Binding Models

As is well-known (Robinson 1981), the cohesive energy of a solid, U_0, is the energy required to disperse its atoms into a dilute, monatomic, gas-like state. For materials evaporating exclusively as atoms, U_0 is the thermodynamic heat of vaporization, corrected to 0 K and zero pressure. For substances containing molecular species in the gas phase, further corrections are needed as well. The energy necessary to remove one atom from an interior (bulk) location in a solid to infinity is $2U_0$, excluding relaxation effects around the residual vacancy. The energy necessary to remove an atom from an average surface site (a 'half-lattice' position) is thus $U_s = U_0$, again ignoring relaxations. These energies are thermodynamic quantities, which apply only when the processes are carried out reversibly: there is no particular reason for the values to be the same when processes are carried out rapidly, as always occurs in sputtering, at least outside the thermal spike regime. It may be noted in passing that a bulk binding energy in a BCA simulation plays somewhat the role of the attractive force in an MD simulation.

In metals, and to a lesser degree in semiconductors, it is plausible to divide the total binding energy into two portions, one localized to the lattice site, the other associated with the crystal as a whole, a model consistent with electrostatic models of a metal surface (Finnis & Heine 1974, Landman et al. 1980). This model is used in both the BC code MARLOWE and the MC code TRIM.SP: the bulk binding energy is often ignored or taken as a small value (Robinson 1983, Eckstein & Biersack 1984), although the value U_0 is indicated by the foregoing discussion and is often used too (Robinson 1990, 1992b). At the surface, the value $U_s = U_0$ is used: since this surface binding energy is regarded as not being localized in interatomic bonds, it is treated as a sort of work function, affecting only the component of a projectile's motion normal to the target surface. This is the well-known planar binding model, widely used in analytical theory (Sigmund 1981, Thompson 1968) as well as in BCA codes.

There are several issues that are not fully resolved. First, U_s ought to depend on the orientation of the crystal surface, but in most calculations this is ignored (appropriately in MC codes). Second, both bulk and surface binding energies ought to depend on the surroundings of an atom: atoms in surfaces or adjacent to defects would be affected. This is not only an issue in prolonged bombardments: in some single cascades, large numbers of atoms can be ejected and changes in binding are surely associated with such events. There is evidence from MD simulations

(Shapiro & Tombrello 1990b, 1991b) that lowering of the surface binding energy by surface disorder is responsible for part of so-called nonlinear effects in sputtering. Thompson (1981) discusses several reasons for such effects. Yamamura (1988) uses a damage-dependent surface binding model in his DYACAT code. Third, both bulk and surface binding could depend on the direction in which an atom recoils. There has been speculation (Garrison et al. 1987, Kelly 1987, Oliva et al. 1987) that U_s should be greater than U_0, but these ideas are based on models in which the surface binding is localized in surface sites or depend on pair-potential calculations by Jackson (1973, 1975), which gave unphysical surface relaxations. See also comments of Andersen (1988).

Recent MD calculations by Gades & Urbassek (1992) have studied the ejection of atoms from a Cu {001} surface using pair potentials and many-body potentials of two types. With a Morse potential, they find the binding energy of an atom in an intact {001} surface to be about 31% greater than U_0, in excellent agreement with calculations of Jackson (1973,1975) and of Lo et al. (1988). However, both EAM and TB potentials gave surface binding energies only about 16% greater than U_0. The EAM result is somewhat lower than was found by Lo et al. (1988). The definition of the surface binding energy differs slightly among these calculations and the two EAM potentials were fit to slightly different data. Gades and Urbassek explain the difference between the pair-potential and many-body potential results in terms of a strengthening of bonds in the target surface, as compared with those in the interior of the target. See Carlsson (1990) for a detailed discussion of bond strengthening at surfaces. The explanation is reminiscent of that of Finnis & Heine (1974) for the inward relaxation of many metal surfaces.

Finally, something must be said about the surface binding model and temporal aspects of sputtering, especially the ejection time. It has been pointed out (Karetta & Urbassek 1992, Hou et al. 1993) that it is difficult to define the time at which an atom is ejected from a target unambiguously and that correlations between the ejection time and other quantities such as the kinetic energies of the sputtered atoms are strongly affected by the definition. The detailed spatial nature of the surface binding process is also an issue. While the energy lost to surface binding is not dependent on the spatial shape of the barrier, the time spent in traversing it is very sensitive to the shape.

6.2 Surface Binding and Sputtered-Atom Energy Spectra

When the planar binding model is used, sputtered atoms lose an energy U_s in passing the binding barrier and, since this energy comes entirely from the velocity component normal to the target surface, experience a refraction as well. The energy

and direction of the sputtered atom are

$$\begin{aligned} E &= E_0 - U_s \\ \mu &= \sqrt{\frac{E_0\mu_0^2 - U_s}{E_0 - U_s}} \end{aligned} \tag{9}$$

where $\mu = \cos\vartheta$, ϑ is the angle between the (outward) surface normal and the atom's velocity, and subscript 0 denotes values before passing the barrier. If the particle flux incident on the binding barrier is isotropic and follows an E_0^{-2} energy spectrum, the sputtered atoms are distributed as

$$p(\epsilon, \mu) = \frac{2S_0}{U_s} \frac{\epsilon\mu}{(\epsilon + 1)^3} \tag{10}$$

where $\epsilon = E/U_s$ and S_0 is the total flux density incident on the barrier in $0 \leq \mu_0 \leq 1$, $1 \leq \epsilon_0 \leq \infty$. Equation (10) is the familiar Thompson model (1968): it has a maximum at $\epsilon^* = 1/2$; the sputtered flux is isotropic (the factor μ is just its projection onto the barrier); and the total flux density of sputtered atoms is $S_0/2$.

Equation (10) can be generalized in a simple way. Sigmund (1981) retained the isotropic flux incident on the barrier, but replaced the energy dependence with the $E_0^{-2(1-m)}$ spectrum appropriate to Lindhard's treatment of scattering (Lindhard et al. 1968), where m is the characteristic power-potential index. Garrison (1986), on the other hand, retained the E_0^{-2} spectrum, but considered the effects of flux anisotropy as a means of obtaining improved agreement with experiments (Baxter et al. 1986) which showed the maximum in the sputtered-atom energy spectrum to vary with direction. These treatments can be unified by specifying the flux incident on the barrier as

$$p_0(\epsilon_0, \mu_0) = (l-1)(k+2)\frac{S_0}{U_s}\frac{\mu_0^{1+k}}{\epsilon_0^l} \qquad 0 \leq \mu_0 \leq 1, \quad 1 \leq \epsilon_0 \leq \infty$$

which may be transformed to give the sputtered flux as

$$p(\epsilon, \mu) = (l-1)(k+2)\frac{S_0}{U_s}\frac{\epsilon\mu}{(\epsilon+1)^{l+1}}\left(\frac{\epsilon\mu^2 + 1}{\epsilon + 1}\right)^{k/2} . \tag{11}$$

Sigmund's result is obtained by setting $l = 2(1 - m)$ and k = 0 and Garrison's by letting $l = k = 2$. Except for the case k = 0, Eq. (11) describes an energy spectrum which depends on the emission direction, or, mutatis mutandis, an angular distribution which varies with the particle energy. Eckstein (1987) has reported TRIM.SP calculations which show sputtered-atom energy spectra which vary with

the direction of emission. The maximum in the energy spectrum is a function of k, l, and μ. Suffice it to say that for $\mu = 1$ (along the target normal), the maximum occurs at $\epsilon^* = 1/l$; for $\mu = 0$, it occurs at $\epsilon^* = 1/(l + k/2)$; and for a range of cases tested, it is a monotonic function of μ. Finally, the fraction of particles incident on the barrier which successfully escape is $(2 + k)/(2l + k)$. This formula, with $k > 0$, can account for BCA simulations which show that substantially more than half the particles incident on the binding barrier with $\epsilon_0 \geq 1$ actually are sputtered. This result is evidently due primarily to the angular distribution of the incident flux and underscores the weakness of the assumption of isotropy.

Whatever the validity of the assumption of isotropic particle fluxes in structureless media, it cannot be satisfactory for atoms ejected from crystalline targets. The focusing effects of the lattice (Lehmann & Sigmund 1966) will alter the angular distributions of the ejecta, as is well known. These effects are clearly displayed by the BCA calculations of Whitlow & Hautala (1987) and of Hou & Eckstein (1990).

The calculations of Gades & Urbassek (1992) reflect on the validity of the planar binding model: they evaluated the refraction of atoms ejected from intact {001} surfaces in Cu at various angles to the surface normal. They find the refraction in a Morse potential to be less than predicted by the planar binding model, whereas the many-body potentials show a greater refraction. Thus, in a Thompson-like model, $\epsilon^* < 1/2$ for the pair potentials and $> 1/2$ for the many-body potentials. These results are consistent with the sputtering simulations of Lo et al. (1988). However, the initial angular and energy distributions of the ejected atoms are decisive in determining the final distributions, so this property alone cannot be used to assess the potentials experimentally.

Another aspect of the planar binding model must also be dealt with by BCA codes. Since some of the atoms incident on the binding barrier have insufficient energy to escape from the target surface, some account of their fates must be given. One possibility, used in TRIM.SP (Biersack & Eckstein 1984), is to allow these atoms to reflect from the barrier and to re-enter the target for further collisions. Another possibility, used in MARLOWE (Robinson 1992a), is to consider such particles as adatoms trapped at the target surface. Since adatom kinetic energies are mostly quite small, the two procedures differ little. A more accurate model could be developed by comparisons with MD calculations.

6.3 Surface Topography and Sputtering Simulation

Sputtering experiments are often performed at doses (fluences) high enough to permit gravimetric determination of the yield. The resulting changes in topography are well-known (Carter et al. 1983, Scherzer 1983). Recent experiments with the scanning tunneling microscope show how topographic features develop even at low

doses from the dynamics of surface vacancies and adatoms (Michely et al. 1991) produced during low-energy ion irradiation of noble-metal surfaces (Michely et al. 1990; Michely & Comsa 1991, 1993; Tsong 1993). Eventually, such features merge into rough surfaces of various kinds (Carter et al. 1983, Scherzer 1983, Eklund et al. 1991). Accounting for the effects of these changes in topography in computer-simulation models is not well advanced.

Yamamura and his coworkers (Yamamura et al. 1987a,b, Yamamura & Muraoka, 1989) used the MC program ACAT (Takeuchi & Yamamura 1983) to study the effects of surface roughness on sputtering simulations. A rough surface was introduced into TRIM (Biersack & Eckstein 1984, Haggmark & Biersack 1981). Several models of roughness were used in these calculations, all on a fairly fine scale. Calculations were made of the dependence of the sputtering yield on the angle of incidence of the ions. This dependence is marked by a maximum yield at an angle of 60° or so from the normal. The angle of the maximum was significantly increased when the surface was roughened, mainly because there was less reflection of the incident particles. The results were in better agreement with experiment than was achieved for smooth targets for 1.05 keV Ar^+ on Ta (Yamamura et al. 1987a) and for 1 keV D on Ni (Haggmark & Biersack 1981). The angles of maximum yield and the effects of roughness on them must depend significantly on the masses of the incident and target particles, crystal orientation, incident energy, and other variables.

The reflection of H atoms from Ni surfaces (Ruzic & Chiu 1989) and the sputtering of graphites by H and C atoms (Ruzic 1990) were studied with a version of TRIM modified to include surface roughness described in terms of fractals. A related fractal surface was also used (Ruzic & Chiu 1989) in a few reflection calculations with an MD code (Baskes 1984) based on the EAM. The fractal TRIM reflection calculations showed a decrease in the reflection coefficient as soon as the fractal dimension D increased above 2, with a minimum around $D = 2.2$, and an increase for larger roughness. The effect was small at normal incidence and most important at grazing incidence. The effect of roughness on the sputtering yield was also small at normal incidence, but, at oblique incidence, the yield increased for small roughness, passed through a maximum, and decreased again for large roughness. The effects were the greatest at the lowest energies.

None of these models of rough surfaces addresses the dynamical evolution of target surfaces during sputtering, although Ruzic's fractal surface model could probably be developed to do this and seems to show promise as part of a model of more realistic surfaces for use in MD and BC calculations. Gades & Urbassek (1992) point out that surface binding energies calculated for intact crystal surfaces are not especially relevant to sputtering under realistic conditions, since atoms in the roughened surfaces will have a statistical distribution of coordination number

and thus will approximate better to the $U_s = U_0$ model.

7 Comparisons of Simulation Models

A few recent investigations compare one simulation model with another or supply information that is relevant to such comparisons. These are useful for understanding the relationships among the different models.

Webb et al. (1986) examined the frequency of encounters between moving particles in cascades, using the QDYN code. A collision was said to occur if the potential energy between two particles exceeded a threshold value. They focused on encounters that were 'nonlinear', that is, in which both colliding atoms were already moving. The number was small at the start of a cascade, but increased to a plateau after 100 to 150 fs, a time corresponding approximately to that at which the maximum number of atoms is in motion, and most particles already have very low energies. In 5 keV Ar^+ bombardments of Cu ~18% of encounters were nonlinear if the threshold was taken as 0.5 eV, ~9% for a threshold of 1 eV, and ~6% for a threshold of 2 eV. These results support the assumption of most BCA codes that encounters between moving particles can often be safely neglected.

Wucher et al. (1992) compare experiments, MD simulations, and BCA simulations of the sputtering of Ni {111} surfaces by 1.1 keV Ar^+. They observed angular distributions of energy-selected sputtered particles. Ejection near a <001> direction was found to be significantly energy-dependent, the maximum moving from a polar angle of 36.3° for 10 eV recoils to 49.4° for 55 eV recoils. Their results are said to be in quantitative agreement with a calculation for Cu (Robinson 1981), based on approximations used in MARLOWE, namely the BCA, the treatment of simultaneous collisions, and the planar surface binding model. The Gibson II Born-Mayer potential (Gibson et al. 1960) was used to describe the interactions of the atoms. The MD simulations of Wucher et al. (1992) used an EAM potential splined to a Molière core (Garrison et al. 1988) and gave a smaller change of the position of the <001> feature with recoil energy. The difference between the two calculations can be attributed partly to different potentials and partly to including the full cascade development in the MD simulation: there are many ways for particles to reach the ejection direction other than the perfectly focused <001> process assumed in the BCA calculation. It must be mentioned that studies of the sputtering of Au {111} surfaces by 0.6 keV Xe^+ with MARLOWE gave quite different results (Hou & Eckstein 1986, Eckstein & Hou 1991). Ejection of target atoms into directions interpreted by Wucher et al. as <011> and <001> directions, are interpreted in terms of other kinds of processes. The differences between these two sets of results is hard to understand. The mass ratios Xe/Au and Ar/Ni are

similar, as are the penetration depths of the ions: for 0.6 keV Xe atoms, the mean penetration into Au {111} targets is $0.867 \pm 0.009\ a_0$ (just over two layers), where a_0 is the lattice constant of Au, 0.4078 nm; for 1.1 keV Ar, the mean penetration into Ni {111} is $1.239 \pm 0.009\ a_0$ (just over three layers), where the lattice constant is 0.3524 nm (Robinson 1992c). Explanations based on traditional focusing processes seem unlikely, but more research is clearly needed.

Chang et al. (1988) compared three methods of simulating the interaction of energetic ions with crystal surfaces, paralleling early work of Karpuzov & Yurasova (1971). One calculation used a full MD treatment of the interaction of Ne ions with Rh {111} and {001} surfaces. A second used a method introduced by Karpuzov and Yurasova in which interactions of the ion with all target atoms are included, but those of the target atoms with each other are ignored. The third was a BCA calculation in which the ion was allowed to interact only with the nearest target atom. In the latter two cases, the scattering of Ar ions from Ni surfaces was also studied. The Molière potential with the Firsov screening length was used for Ne-Rh and Ar-Ni interactions; the Rh-Rh interactions were described by a Morse potential splined to a Molière core. Chang et al. report angular and energy distributions for backscattered particles. In agreement with Karpuzov and Yurasova, they find very close agreement between the first two models, except at low energies (100 eV Ne on Rh {001}) where deviations begin to appear. Substantial differences are reported for the BCA model, however. These depend in a complex way on the incidence conditions (energy, polar and azimuthal angles) and on the surface. The conclusions agree generally with those of Karpuzov and Yurasova, who mainly analyzed trajectories. Both comparisons show the severe limitations of a BCA model which does not include any correction for nearly simultaneous encounters of projectiles with several target atoms. Comparisons using, for example, the MARLOWE approximations (Hou & Robinson 1976, Robinson 1989, 1993) could further illuminate this issue.

Shulga et al. (1989) used an MD simulation to examine the trajectories of particles during the scattering of heavy atoms from diatomic molecules made up of lighter atoms, using the example of Xe on Cu_2. In such cases, the first atom of the molecule may move out ahead of the heavy projectile, clearing the way for it by displacing the other member of the molecule before the heavy particle arrives. Comparisons of trajectories where the interactions of the target atoms with each other were included with those in which they were suppressed showed the importance of such effects. Smith & Webb (1992) have also noted the importance of time in the proper ordering of collisions. They show examples of how some BCA models can go astray, as compared with MD models.

The most extensive comparison of computer simulation models is the recent round-robin evaluation of the ejection probability of low-energy atoms near the

surfaces of crystals (Sigmund et al. 1989). This work compared six MD codes (Harrison 1988, Valkealahti & Nieminen 1987, Baskes 1984, Shulga 1980, Chakarov & Karpuzov 1988, Shapiro & Tombrello 1987), four BC codes (Robinson 1989, Yamamura & Takeuchi 1987, Hautala 1984, Shulga 1983), and eight MC codes (Takeuchi & Yamamura 1983, Vicanek & Urbassek 1988, Hautala 1980, Betz et al. 1971, Kang et al. 1985, Ishitani et al. 1983, Cui & Li 1985, Biersack & Eckstein 1984). The task was to calculate the probability of ejection of atoms from the surface region of Cu targets as a function of depth within the target and the initial direction and kinetic energy of the recoil. The Gibson II Born-Mayer potential (Gibson et al. 1960) was used for most calculations. The planar surface binding model was used in most BCA calculations. There were substantial discrepancies among the results of the various codes for the relatively simple process examined. Some of these were merely statistical, while others could be traced to the details of the programs themselves. The lattice models, that is, the MD and BC codes, agreed among themselves reasonably well, although the neglect, or, rather, the very approximate treatment, of many-body effects in the latter caused differences to increase at low energies. The lattice models differed systematically from the MC models, however. The former agreed that no ejection of atoms occurred from below the second or third layer of the targets (never from depths as great as 0.4 nm), for primary energies up to 50 eV. The MC codes, on the other hand, showed ejection from depths of 0.4 to 0.5 nm, even at energies as low as 10 eV. Moreover, there were considerable variations among the different programs. Much of the variation was traced to detailed features of the individual models: the original work (Sigmund et al. 1989) should be consulted for these and other topics. The general differences between the lattice models and the MC models result from the statistical nature of the latter. Their rough surfaces and lack of translational symmetry result in emission from depths greater than is possible in the lattice codes. Similar effects would appear in the lattice models if thermal displacements of the atoms from their lattice sites were introduced.

8 The Statistics of Sputtering

No sputtering experiment has been carried out at a dose rate small enough to allow the observation of fluctuations in the yield of ejected particles between different incident ions. A few observations of small pits on sputtered surfaces (Merkle & Jaeger 1981) are regarded as resulting from single ion impacts, but these presumably record only extreme fluctuations. Simulations easily record detailed distributions of sputtering yields and allow evaluation of the mean yield and of higher moments. Attention to the statistics of sputtering and to the closely-related topic

of correlations between the ion impact point and the yield allow statements to be made about mechanisms which influence the yield and about conditions which are likely to favor the ejection of molecular clusters or the development of pits and other topographic features on the irradiated surface. In addition, from the statistics of yield fluctuations, the precision of computations may be assessed directly in objective terms.

8.1 The Number of Displaced Atoms

Statistical studies of many aspects of collision cascade development are accessible to computer simulation and, in some cases, allow assessment of analytical models. For example, Kinchin & Pease (1955a,b) evaluated the mean number of Frenkel-defect pairs produced in a structureless medium by a primary recoil of initial kinetic energy E as

$$\langle \nu \rangle = \frac{E}{2E_d} \qquad E > 2E_d$$

where ν is the number of defects, E_d is the displacement threshold energy, and $<>$ indicates averaging. Hard-core scattering was assumed and electronic energy losses were ignored. Leibfried (1958, 1965) showed that the corresponding variance was

$$\sigma^2 = < (\nu - \langle \nu \rangle)^2 > = (4 \ln 4/3 - 1) \langle \nu \rangle \qquad E > 4E_d \tag{12}$$

where the numerical factor has the value 0.150728. Only the high-energy forms of these equations are shown; for more details see Leibfried (1965). Equation (12) shows that the variance is only 15% of the Poisson value. The smallness of the variance was confirmed by computer simulation (Robinson & Torrens 1974), but the energy dependence in Eq. (12) is overwhelmed by damage-energy straggling.

8.2 The Sputtering Yield

In striking contrast, sputtering yields are distributed over a wide range and the mean often bears little relationship to the most probable yield. Studies of the statistics of sputtering are available from MC codes (Eckstein 1988, 1991; Hou & Eckstein 1992; Conrad & Urbassek 1990), BC codes (Robinson 1983), and MD codes (Harrison 1981b, 1988, Harrison & Webb 1982, Harrison et al. 1987, Smith & Harrison 1989, Stansfield et al. 1989). Systematic differences are found between yield distributions from monocrystalline targets and from polycrystalline and structureless targets. The latter show a mode (most probable value) in the vicinity of the mean and a broad distribution that can be fit by a negative binomial distribution (Eckstein 1988, 1991), although there is disagreement about this (Conrad & Urbassek 1990). In monocrystal targets, on the other hand, BC and MD calculations

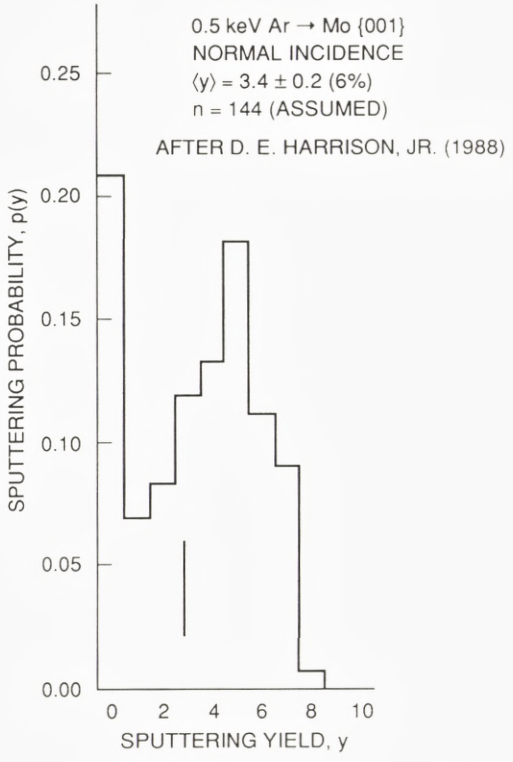

Figure 5. The sputtering yield distribution for 0.5 keV Ar on a Mo {001} surface. The data are taken from Fig. 14 of Harrison (1988). The figure is constructed on the assumption that there were 144 incident particles in the sample: with this choice, there is one count in the right-most channel. A vertical line in the histogram marks the mean yield.

agree in finding a significant probability that the incident particle ejects no target atoms at all, a probability that increases with the incident kinetic energy and is unquestionably associated with channeling of the incident beam in low-index axial and planar channels of the target. The remainder of the distribution in monocrystal targets resembles that found in structureless and polycrystalline ones.

Let $p(y)$ be the probability, normalized to unity, that an incident ion ejects exactly y atoms from a target. The sputtering yield is the mean value

$$Y = \langle y \rangle = \sum_{y=0}^{\infty} y p(y) \; ;$$

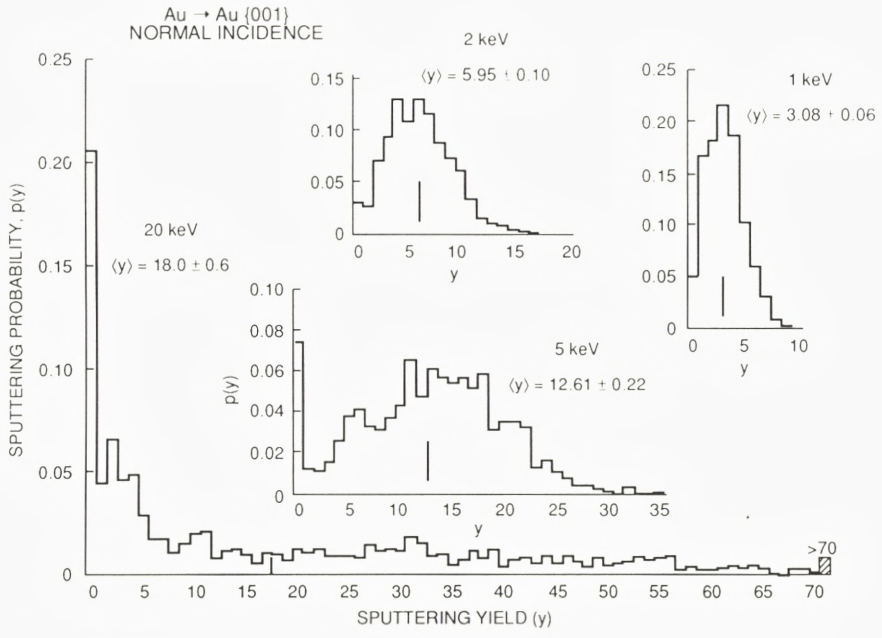

Figure 6. Sputtering yield distributions for Au atoms normally incident on a Au {001} surface, evaluated with MARLOWE (Robinson 1992c). A vertical line in each histogram marks the mean yield.

other moments are similarly defined. The variance of the yield is

$$\sigma^2 = \langle (y - \langle y \rangle)^2 \rangle \ ;$$

other central moments are similarly defined. If y is a random variable, $\langle y \rangle$ is expected from the central limit theorem (Feller 1957) to obey a normal distribution with variance $\sigma^2/(n-1)$, where n is the number of incident ions. This prediction of the central limit theorem applies to the distribution of mean values $<y>$, each from an independent sample of n incident ions. No assumption is required about $p(y)$, the distribution of single-ion yields. These results allow an assessment of the precision attained in calculations, especially important with MD models, where the sample sizes are generally small.

Figure 5 shows a yield distribution calculated by MD for 0.5 keV Ar atoms normally incident on a Mo {001} surface (Harrison 1988). The usual procedure in Harrison's calculations was to divide the asymmetric surface cell into a number (here deduced to be 144) of equal parts and to select an impact point randomly

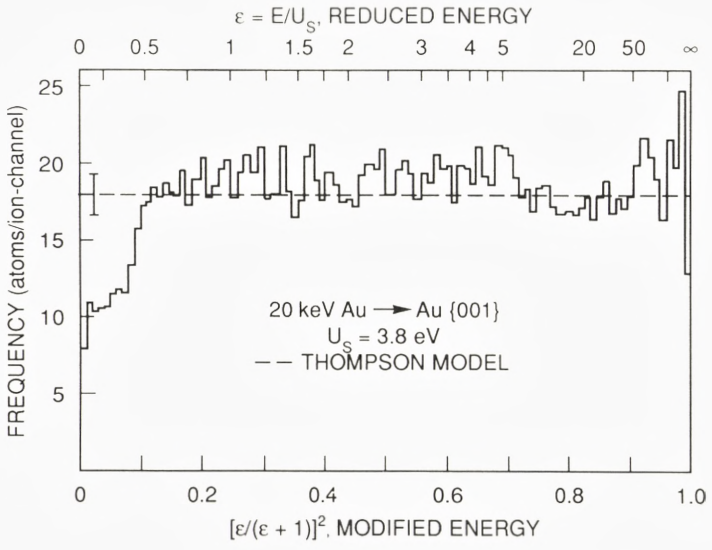

Figure 7. The energy spectrum of sputtered atoms evaluated with MARLOWE (Robinson 1992c) for 20 keV self-sputtering of Au {001}. The prediction of the Thompson (1968) model is shown by the horizontal dashed line; the statistical uncertainty of this value is shown.

within each one. The incident particles were then launched on trajectories aimed at these impact points. It is stated (Harrison 1988) that different sets of impact points selected in this manner gave results which agreed always to 'within 10% and almost always within 5%.' As Fig. 5 shows, however, the standard error of the yield, evaluated on the assumption that y is a random variable, is 6%. It is concluded that the precision of such MD calculations is just that which would be deduced for a sample selected by ordinary aleatory methods. In conventional sampling theory (see, for example, Feller 1957), one would expect the means of replicate samples of the type shown in Fig. 5 to deviate by less than 6% about two-thirds of the time and to deviate by more than 12% less than 5% of the time. This is simply a quantification of the quotation cited. Thus, Harrison's method of ensuring uniformity of irradiation actually gives results no better than do purely aleatory methods, although it may reduce the risks of large fluctuations associated with small sample sizes. This being the case, the question (Andersen 1987) whether the yield is a smooth or a chaotic function of the impact point is less important than it might be otherwise. It has, indeed, never been shown what the situation really is and this could bear on several issues, especially those involving correlations of the impact point with quantities other than the yield.

Figure 6 shows the incident-energy dependence of yield distributions evaluated with MARLOWE (Robinson 1992c) for Au normally incident on Au {001}. Each sample included 1000 incident particles. The larger samples give better precision than was achieved in Fig. 5, but the results are similar. The <001> axial channel opens rapidly above 2 keV; by 20 keV, fully 20% of the incident particles cause no sputtering at all. The occurrence of events in which the number of ejected atoms is much larger than the mean value should be noted. At 20 keV, yields extend to values > 90 with a small incidence. While nothing is known about such events from these calculations, it is natural to look at them as likely sources of cluster emission and surface pit formation, which was observed in MD simulations (Harrison 1988, Stansfield et al. 1989, Wucher and Garrison 1992), although most of these were restricted to rather low kinetic energies.

It would be desirable to have detailed studies of correlations of the sputtering yield with the impact point of the incident particle, beyond delimiting the channels by low- or non-yield situations. Harrison (1988) has reported a correlation of this kind for 0.5 keV Ar on a Rh {111} surface, but the results are very hard to interpret (see his Fig. 11). Such studies could determine whether the yield is indeed a smooth or a chaotic function of the impact point (Andersen 1987) and should be useful in understanding other kinds of correlations.

Other kinds of correlations can also be studied. As an example, Hou & Eckstein (1992) have reported correlations of the single-particle yield y [see Eqs. (27-29)] with the total number of atoms displaced in a cascade, the sputtered energy distribution, and the surface deposited energy, using the TRIM.SP code. They used these results to discuss the connection between the surface deposited energy and the yield.

8.3 Other Distributions

In view of what was said above about the precision of sputtering yield calculations, it is appropriate to make a few remarks about the precision of calculated sputtered-atom energy spectra, angular distributions, and the like. It should be clear that definitive data about such distributions can be obtained only from computational samples of sufficient size. With small samples, especially when the yield is small, only very approximate distribution functions can be obtained. However, some questions can be addressed more reliably by careful selection of the statistic to be examined.

For example, the validity of the Thompson model for the angle-averaged energy spectrum of the sputtered particles may be tested by constructing a histogram based, not on the sputtered atom's kinetic energy, but on the dimensionless modi-

fied energy variable $[\epsilon/(\epsilon+1)]^2$, where $\epsilon = E/U_s$. Since

$$d\left(\frac{\epsilon}{\epsilon+1}\right)^2 = \frac{2\epsilon d\epsilon}{(\epsilon+1)^3}$$

it follows that such a histogram will have equal counts in each channel (except the last) if the Thompson model is obeyed and will deviate otherwise. Figure 7 shows such a modified-energy histogram for the self-sputtering of Au {001} at 20 keV, evaluated with MARLOWE (Robinson 1992c). The number of atoms with energies $< U_s/2$ is significantly less than predicted by the Thompson model, but this is compensated by a slight excess at energies up to about 6 U_s; a small deficit appears around 10 U_s and an excess at the highest energies. These features can be seen much more clearly in the modified histogram than would be possible in a simple energy spectrum. Such techniques can often be used to improve the reliability of interpreting noisy data.

9 Cluster-Ion Impacts

There has been an interest in sputtering by molecules since experiments demonstrated that the yield per atom is often greater for diatomic ions than for monatomic ones, especially for high-energy heavy ions on heavy targets (Andersen & Bay 1981, Andersen 1993). Shapiro & Tombrello (1990b, 1991b) simulated impacts of some monatomic and diatomic ions on Cu and Au crystals using the SPUT2 code (Shapiro et al. 1988). At incident kinetic energies of 5 keV/atom, they found statistically significant nonlinearities in the yields for Kr and Xe ions on Cu {001} and for Kr, Xe, Au, and U ions on Au {001} and {111}, but not for Ar and Cu ions on Cu {001}. They attributed these results to collision spikes involving encounters between moving recoils, with a secondary contribution from changes in the surface binding energy caused by collisional disruption of the surface. Broomfield et al. (1990) simulated the sputtering of Cu {001} by $SiCl_4$ ions at incident energies up to 800 eV. Above the very low energy of $\sim$ 50 eV, they found nonlinearities in the yield, attributed to lowering of the surface binding energy by disruption of the target surface. Taken together, these simulations suggest that sputtering nonlinearities result from surface disruption and from spike effects, the relative importance of the two mechanisms depending on the targets, the atoms in the incident clusters, the energies of the particles, and the sizes of the clusters.

There is much current interest in the impacts of large cluster ions on solid surfaces. The incident particles are singly-charged clusters of as many as several hundred or even a few thousand atoms, with initial kinetic energies from $<$ 1 eV/atom to $\sim$ 1 keV/atom or more. The interest in such particles stems from their

potential uses in forming thin films by the ionized cluster beam (ICB) technique (see Brown et al. 1991 for a review); from claims of nuclear fusion during impacts of large, slow D_2O clusters on deuterated solid targets (Beuhler et al. 1989, 1990; Bae et al. 1991; but see Fallavier et al. 1990 for negative results and Beuhler et al. 1992 for withdrawal of the original claim); and from interest in other impact phenomena (Beuhler & Friedman 1986). Such impacts have also been suggested as a means of carrying out exotic chemical reactions in the clusters (Cleveland & Landman 1992). Sigmund (1989) discussed some of the features that can be expected in cluster impacts, but simulation methods are especially attractive for assessing the possibilities. The atomistic simulation of cluster impacts is feasible as long as the events can be contained adequately. This suggests limits ~10 eV/atom for clusters of a few hundred atoms or clusters of a few tens of atoms at 1 keV/atom. For extremely large clusters, it would surely be more effective to use models based on macroscopic mechanics.

The first simulation of ICB deposition appears to be that of Mueller (1987), a two-dimensional calculation using Lennard-Jones potentials. Incident kinetic energies ranged from 0.1 to 1.5 in units of the well-depth in the potential. Since well-depths are ~ 1 eV, these calculations correspond to very low energies. Biswas et al. (1988) and Kwon et al. (1990) used the empirical many-body potential of Biswas & Hamann (1987) in simulations of Si-cluster impacts on Si {111} surfaces. The clusters were mainly amorphous Si_{33} with energies from 0.23 to 1.4 eV/atom. The emphasis in this work was on film growth and the conditions for obtaining amorphous or epitaxial films. The energies are low enough that there is little penetration of cluster atoms into the targets.

Yamamura (1988) developed DYACAT for cluster impact studies, applying it initially to the sputtering of amorphous C by Ar clusters with 10 to 200 atoms at an initial energy of 100 eV/atom. He later studied the ICB deposition of Ag clusters with 100 to 500 atoms on amorphous C at energies of 6 to 10 eV/atom (Yamamura 1990); the atomic kinetic-energy spectra during impacts of Ag and Al clusters with 10 to 500 atoms on amorphous C and Au, at energies up to 1 keV/atom (Yamamura 1991); and the angular distributions of sputtered atoms during irradiation of Al and Ag by 1- to 500-atom clusters of Ag and Al, respectively (Yamamura & Muramoto, 1993). In these calculations, there is often substantial penetration of cluster atoms into the substrate. As the incident particles slow down in the targets, the atoms at the front of the cluster slow down before the arrival of the trailing parts. As a result of collisions between cluster atoms, some are accelerated to speeds well in excess of the initial values. In addition, lattice atoms are displaced and run ahead of the advancing cluster atoms. This is the 'clearing the way' effect (Sigmund 1989). One consequence is that the rates of energy loss of many cluster atoms is substantially less than that of isolated atomic particles.

In addition, there are substantial nonlinearities in sputtering yields, even at low kinetic energies, and significant cratering of the targets on a scale larger than the sizes of the clusters. These effects are largest when the incident atoms are heavier than the target atoms. Yamamura's calculations show the distortion of the cluster as it impacts a surface at low energy, but cannot deal effectively with spreading of the cluster or its conversion to a surface film.

Sigmund and his coworkers used a metastable MD model (Shulga 1980, Shulga et al. 1989) for studies of cluster impacts. Born-Mayer potentials with the parameters of Andersen & Sigmund (1965) were used, truncated to avoid premature 'explosion' of the clusters and targets under the conditions of the calculations, which addressed primarily the slowing down of cluster atoms in thin polycrystalline targets. The systems studied included 0.1 and 1 keV/atom Au_{13} impacting Si (Shulga & Sigmund 1990); 0.1 keV/atom C clusters with 1 to 17 atoms on Au (Pan & Sigmund 1990); 0.1 and 1 keV/atom Cu_{13} on Cu (Shulga 1991); 0.1 keV Cu_{13} on Au (Shulga & Sigmund 1991) and 0.1 and 1 keV/atom Au clusters with 1 to 34 atoms on Au (Pan 1992). These calculations show that, when the incident atoms are heavier than the target atoms, the front runners (it is difficult to avoid an analogy with the linemen in rugby or American football) accelerate some target atoms to speeds greater than that of the incident atoms, allowing later atoms in the cluster to penetrate more deeply into the target before encountering target atoms. The average energy loss per atom of the incident clusters is less than experienced by atomic particles. Similar effects persist even in the equal-mass cases. When the cluster atoms are lighter than the target atoms, their backscattering leads to collisions among cluster atoms which can be described as collision cascades occurring in the clusters. In addition, target atoms can be hit by more than one cluster atom. At all mass ratios, combinations of these effects cause broadening of energy spectra and the generation of particles moving faster than expected from two-body kinematics. There are significant effects on particle reflection and sputtering, but these calculations cannot deal completely with the latter.

The SPUT2 code (Shapiro et al. 1988) has been used to study cluster impact phenomena. The atomic interactions were based on Morse potentials splined to Molière cores. Since the clusters and the targets are stable, such simulations are suitable for problems where metastable models cannot be used. Studies were made of impacts of 1 keV/atom Al, Cu, Au, and composite clusters with 32 or 63 atoms on Al, Cu, and Au {001} targets (Shapiro & Tombrello 1990a, 1991a). Evolution of the systems was followed for 0.5 ps, long enough to make clear many features of the impacts, but not long enough to produce reliable estimates of sputtering yields. As the cluster hit the target, the atomic density in the primary impact-zone rose rapidly to about twice its initial value and then fell rapidly, reaching its original value in $\sim$30 fs. As material was ejected from the target or driven into

it, the density in the primary impact-zone then fell to about 25% of its original value over 100 fs. Potential-energy spectra of the atoms showed that during the first 60 fs some were accelerated to energies considerably higher than expected from two-body kinematics, in agreement with the results of the Sigmund group, and the associated 'clearing the way' was also seen. An interesting feature of these calculations was seen in distributions of the sites from which the sputtered atoms originated. These showed few atoms to come from the core of the impact zone, but, instead, there was a ring of emission surrounding the core, closely resembling the splash seen when heavy objects impact liquids.

The excitation of core electrons was studied during impacts of 0.2 to 1 keV/atom Al and composite clusters with 32, 63, or 108 atoms on Al {001} targets (Shapiro & Tombrello 1992a,b). The composite clusters consisted of three layers (38 atoms) of Al backed by two layers (25 atoms) of Au. A critical approach distance was used to define L-shell excitation in the Al atoms. During the initial rapid compressional phase, significant excitation was found above a threshold energy of ~0.4 keV/atom for Al clusters and ~0.11 keV/atom for composite clusters. Intermediate-size clusters produced core excitations most efficiently. This was attributed to greater 'clearing the way' effects with the largest clusters. The authors suggest experimental studies of Auger emission from core excited states as a probe of the early compressional phase of cluster-ion impacts.

Studies were made at 1 to 10 eV/atom of the final shapes and penetration depths of 63 atom Al and Au clusters on Au {001} (Pelletier et al. 1992). The simulations extended for 2 ps after impact. The barycenter of the Al clusters never penetrated the gold target at these low energies, but the most energetic Au cluster did penetrate slightly. All clusters were flattened substantially. At low energies, the films were in good registry with the substrate, but at higher energies, the registration was poor and there was much damage to the target.

Studies have also been carried out of Cu, Ni, and Al clusters of 4 to 92 atoms impacting the same metals at energies up to 1 keV (Hsieh & Averback 1990, Averback et al. 1991, Hsieh et al. 1992). EAM potentials with Molière cores were used in these calculations. The simulations extended to as long as 20 ps after the impact. The behavior depended sensitively on the size and energy of the cluster, the masses of the cluster and target atoms, and the properties of the substrates as modelled by the EAM potential. An important feature of these calculations is that they show very little mixing between the atoms of the cluster and those of the substrate. This behavior supports the idea of using macroscopic modelling of many aspects of cluster impacts. As a 326 eV Cu_{92} cluster begins to impact a Cu surface, the substrate is initially compressed, but, after ~0.7 ps, begins to rebound; the maximum expansion occurs at about 1 ps; after ~2.4 ps, the atoms begin to relax towards their final positions; and, by ~5.5 ps, all atoms have settled onto

lattice sites. Little damage is produced in the targets. At the end of the impact, a ridge of substrate atoms appears on the surface, surrounding the impact zone. The interpretation is that the shear stress generated in compressing the substrate exceeds the critical shear strength of the target and, during the subsequent expansion, atoms flow out onto the surface. A 326 eV Cu_{92} cluster impacts a Ni target in a similar way, but penetrates less far into the substrate and the ridge of substrate atoms is less pronounced. This is consistent with the greater strength of Ni. When the cluster energy is increased to 1 keV, the plastic response of the substrate is more pronounced, but there is still little mixing of cluster and substrate atoms during the compression phase. There is also evidence of local melting in this impact and a few vacancies appear in the substrate when the melted zone is quenched. When smaller clusters of the same energy were used, such as 326 eV Cu_{13} or Cu_4, craters were produced at the target surfaces. A few interstitial atoms were produced deep within the substrate by the smallest cluster.

By combining results for various clusters and substrates, it was possible to deduce a sort of 'phase diagram,' with two variables: the kinetic energy per cluster atom and the cluster cohesive energy, each normalized to the cohesive energy of the substrate. When the former is > 10, implantation of the clusters and radiation damage to the substrate occur. When it is ~ 1, the clusters remain intact, forming a 'glob' of material on the surface if the substrate is hard, or penetrating it if it is soft. At intermediate energies, the cluster breaks up on hitting hard substrates, spreading out over the surface, dissociating, and being reflected from it. Intermediate-energy clusters penetrate soft substrates and induce local melting. These results are generally consistent with those cited earlier, but each group has concentrated on a different aspect of the cluster impact problem. It would be interesting to make more detailed comparisons of impacts simulated by different investigators, in order to rationalize the various viewpoints more completely and to understand how much the differences in modelling affect the results.

Mention must also be made of a recent simulation of the impact of a 561-atom Ar cluster on a rock-salt surface at an energy of $\sim$ 1.9 eV/atom (Cleveland & Landman 1992). The Ar atoms interacted with each other through Lennard-Jones potentials with a well-depth of 10.3 meV, and with the atoms of the substrates through the potentials of Ahlrichs et al. (1988); the substrate atoms interacted with each other through the potentials of Catlow et al. (1977). The authors describe their event in terms similar to those used by Hsieh et al. (1992). The Ar cluster retains its identity up to about 0.5 ps, but then disrupts. As in earlier calculations, a compression of the substrate and the cluster is observed for $\sim$ 0.5 ps, followed by an expansion. Whether it is appropriate to describe such a short pressure pulse as a 'shock' may be argued, but its occurrence is clear enough.

Finally, some interesting simulations have been reported for buckminsterfull-

erene (C_{60}) molecules incident on hydrogen-covered diamond surfaces (Mowrey et al. 1991) and graphite (Smith & Webb 1993). In the former case, the potential was of the Tersoff type, with special modifications to fit various chemical effects (Brenner 1990); the latter calculations used a carbon potential of Tersoff (1988b). An interesting feature of both calculations is that at incident energies $\lesssim$ 4 eV/atom, the C_{60} molecules rebound from the surface intact, although with substantial internal energy. Whether these would eventually fragment, as seems to occur for sputtered metal clusters (Wucher & Garrison 1993) is not yet settled, although it seems likely.

10 Concluding Remarks

I have tried in this review to consider several of the incomplete issues raised by Andersen (1987) in his earlier survey. The current situation with respect to potential functions has been discussed, both for close approaches between atoms and for separations near the normal bonding distances in solids. Methods of determining the former from ab initio calculations appear to be more-or-less in hand and empirical potentials for the latter are well-advanced. The role of electron excitations in slowing swift particles has been outlined and methods of including such effects in simulation codes have been discussed. It was pointed out that the role of electronic energy losses at low energy is still ambiguous and that more work is needed to clarify the part played in sputtering by electron-phonon interactions. The modelling of crystal surfaces has been discussed, as well as the influence of the surface on sputtered particle angular and energy distributions. It was pointed out that the effects of prolonged irradiation need to be included in simulations intended to model real experimental situations.

Limited comparisons of codes of different types have been presented. More work in this area would be very desirable. This could relate MD, BC, MC, and intermediate codes in the way done in the recent round-robin collaboration (Sigmund et al. 1989), but should be applied to a variety of problems. The statistics of sputtering were discussed: it is to be hoped that more attention will be given to statistical aspects of MD simulations, since they are usually run with very small sample sizes. Finally, recent work on cluster impacts was surveyed with the idea of giving some of the flavor of this recently active field. Further work in this area appears warranted.

Several topics in the computer simulation of of ion-solid interactions have been omitted. Many are reviewed elsewhere in this volume. One such topic is the ejection of molecular species during sputtering, which is reviewed by Urbassek & Hofer (1993). The related topic of the ejection of very large molecules by swift ion

bombardment is reviewed by Reimann (1993).

No attention has been paid to the sputtering of multicomponent targets, technologically a very important topic. In addition to the issues raised in simulating the sputtering of single component materials, there are additional major issues in multicomponent ones. The most significant are concerned with the selective sputtering of the components and the accompanying changes in composition, binding energies, and the like. In prolonged irradiations, diffusion effects may be superadded. A recent example of work in this field is given by Baretzky et al. (1992). See Betz & Wehner (1983) and Lam & Sigmund (1993) for reviews of multicomponent sputtering and Sigmund (1987a) for some analysis of the subject.

Acknowledgements

I have had invaluable help in preparing this article from discussions with several colleagues, sometime in person, sometimes by electronic communication. I especially want to thank Gerhard Betz, Wolfgang Eckstein, S. H. Liu, Mark Shapiro, Peter Sigmund, Roger Smith, and Roger Webb. It would not have been possible to complete work on the manuscript successfully without the advice and invaluable assistance of Marc Hou.

This research was sponsored by the Division of Materials Sciences, U. S. Department of Energy under Contract No. DE-AC05-84OR21400 with Martin Marietta Energy Systems, Inc.

References

Abraham FF, 1986: Adv. Phys. **35**, 1

Abraham FF and Batra IP, 1985: Surface Sci. **163**, L752

Adams JB and Foiles SM, 1990: Phys. Rev. B **41**, 3316

Ahlrichs R, Boehm HJ, Brode S, Tang KT and Toennies, JP, 1988: J. Chem. Phys. **88**, 6290

Allen MP and Tildesley DJ, 1987: *Computer Simulation of Liquids* (Clarendon Press, Oxford)

Andersen HH, 1987: Nucl. Instrum. Methods B **18**, 321

Andersen HH, 1988: Nucl. Instrum. Methods B **33**, 466

Andersen HH, 1993: K. Dan. Vidensk. Selsk. Mat. Fys. Medd **43**, 127

Andersen HH and Bay HL, 1981: *Sputtering by Particle Bombardment I*, edited by R Behrisch (Springer, Berlin) 145

Andersen HH and Sigmund P, 1965: Nucl. Instrum. Methods **38**, 238

Antonov SL, Ivanov IN, Orlikovsky AA, Vasil'chenko VYu and Yurasova VE, 1990: Nucl. Instrum. Methods B **48**, 553

Aono M, 1984: Nucl. Instrum. Methods B **8**, 374

Averback RS, Diaz de la Rubia T and Benedek R, 1988: Nucl. Instrum. Methods B **33**, 693

Averback RS, Diaz de la Rubia T, Hsieh H and Benedek R, 1991: Nucl. Instrum. Methods B **59/60**, 709

Azziz N, Brannon KW and Srinivasan GR, 1985: Materials Research Society Symposia Proceed-

ings **45**, 71
Azziz N, Brannon KW and Srinivasan GR, 1987: Phys. Stat. Sol. (b) **142**, 35
Bae Y, Lorentz DC and Young SE, 1991: Phys. Rev. A **44**, R4091
Barat M and Lichten W, 1972: Phys. Rev. A **6**, 211
Baretzky B, Moeller W and Taglauer E, 1992: Vacuum **43**, 1207
Barrett JH, 1990: Nucl. Instrum. Methods B **44**, 367
Baskes MI, 1984: J. Nucl. Mater. **128/129**, 676
Baskes MI, 1987: Phys. Rev. Lett. **59**, 2666
Baskes MI, 1992: Phys. Rev. B **46**, 2727
Baxter JP, Singh J, Schick GA, Kobrin PH and Winograd N, 1986: Nucl. Instrum. Methods B **17**, 300
Betz G and Wehner GK, 1983: *Sputtering by Particle Bombardment II*, edited by R Behrisch (Springer, Berlin) 11
Betz G, Dobrozemsky R and Viehboeck FP, 1971: Int. J. Mass Spectrom. Ion Phys. **6**, 451
Betz G, Pellin MJ, Burnett JW and Gruen DM, 1991: Nucl. Instrum. Methods B **58**, 429
Beuhler RJ and Friedman L, 1986: Chem. Rev. **86**, 521
Beuhler RJ, Friedlander G and Friedman L, 1989: Phys. Rev. Lett. **63**,1292
Beuhler RJ, Friedlander G and Friedman L, 1992: Phys. Rev. Lett. **68**, 2108
Beuhler RJ, Chu YY, Friedlander G, Friedman L and Kunnmann, W,1990: J. Phys. Chem. **94**, 7665
Biersack JP, 1987: Nucl. Instrum. Methods B **27**, 21
Biersack JP and Eckstein W, 1984: Appl. Phys. A **34**, 73
Biswas R and Hamann DR, 1987: Phys. Rev. B **36**, 6434
Biswas R, Grest GS and Soukoulis CM, 1988: Phys. Rev. B **38**, 8154
Bohr N, 1915: Phil. Mag. (6) **30**, 581
Brandt W and Kitagawa M, 1982: Phys. Rev. B **25**, 5631
Brenner DW, 1990: Phys. Rev. B **42**, 9458
Brenner DW and Garrison BJ, 1986: Phys. Rev. B **34**, 1304
Broomfield K, Stansfield RA and Clary DC, 1988: Surface Sci. **202**, 320
Broomfield K, Stansfield RA and Clary DC, 1990: Surface Sci. **227**, 369
Brown WL, Jarrold MF, McEachern RL, Sosnowski M, Takaoka G, Usui H and Yamada I, 1991: Nucl. Instrum. Methods B **59/60**, 182
Burenkov AF, Komarov FF and Kumakhov MA, 1980: Phys. Stat. Sol. (b) **99**, 417
Carlson TA, Lu CC, Tucker TC, Nestor CW, Jr and Malik, FB, 1970: U.S.A.E.C. Report ORNL-4614
Carlsson AE, 1990: Solid State Physics **43**, 1
Caro A and Victoria M, 1989: Phys. Rev. A **40**, 2287
Caro A, Victoria M and Averback RS, 1990: J. Mater. Res. **5**, 1409
Carter G, Navinšek B and Whitton JL, 1983: *Sputtering by Particle Bombardment II*, edited by R Behrisch (Springer, Berlin) 231
Catlow CRA, Diller KM and Norgett MJ, 1977: J. Phys. C: Solid State Phy. **10**, 1395
Chakarov IR and Karpuzov DS, 1988: unpublished
Chandrasekhar S, 1943: Rev. Mod. Phys. **15**, 1
Chang CS, Knipping U and Tsong IST, 1986: Nucl. Instrum. Methods B **18**, 11
Chang CS, Knipping U and Tsong IST, 1987: Nucl. Instrum. Methods B **28**, 493
Chang CC, Winograd N and Garrison BJ, 1988: Surface Sci. **202**, 309
Chaplot SL, 1988: Phys. Rev. B **37**, 7435
Chaplot SL, 1989: Phase Transitions **19**, 49
Chaplot SL, 1990: Phys. Rev. B **42**, 2149
Chen SP, Voter AF and Srolovitz DJ, 1986: Phys. Rev. Lett. **57**, 1308

Chen SP, Voter AF, Albers RC, Boring AM and Hay PJ, 1990: J. Mater. Res. **5**, 955
Chini TK and Ghose D, 1989: Nucl. Instrum. Methods B **42**, 293
Chou SP and Ghoniem NM, 1991: Phys. Rev. B **43**, 2490
Cleveland CL and Landman U, 1992: Science **257**, 355
Conrad U and Urbassek HM, 1990: Nucl. Instrum. Methods B **48**, 399
Cowern NEB and Biersack JP, 1983: Nucl. Instrum. Methods **205**, 347
Cui FZ and Li HD, 1985: Nucl. Instrum. Methods B **7/8**, 650
Cui FZ, Xie J and Li HD, 1992: Phys. Rev. B **46**, 11182
Cyrot-Lackmann F, 1968: J. Phys. Chem. Solids **29**, 1235
Daw MS and Baskes MI, 1984: Phys. Rev. **29**, 6443
Diaz de la Rubia T and Guinan MW, 1990: J. Nuclear Mater. **174**, 151
Diaz de la Rubia T and Guinan MW, 1991: Phys. Rev. Lett. **66**, 2766
Diaz de la Rubia T, Averback RS, Benedek R and King WE, 1987: Phys. Rev. Lett. **59**, 1930
Diaz de la Rubia T, Averback RS, Hsieh H and Benedek R, 1989: J. Mater. Res. **4**, 579
Diaz de la Rubia T, Averback RS, Benedek R and Robertson IM, 1990: Radiat. Eff. **113**, 13
Dodson BW, 1987a: Phys. Rev. B **35**, 2795
Dodson BW, 1987b: Phys. Rev. B **36**, 1068
Dodson BW, 1987c: Appl. Surface Sci. **29**, 334
Dodson BW, 1989: Mater. Res. Soc. Symposium Proc. **128**, 137
Dodson BW, 1990: Nucl. Instrum. Methods B **44**, 273
Dodson BW, 1991: Nucl. Instrum. Methods B **59/60**, 481
Dodson BW and Taylor PA, 1987: J. Mater. Res. **2**, 805
Ducastelle F, 1970: J. Phys. (Paris) **31**, 1055
Echenique PM, Nieminen RM and Ritchie RH, 1981: Solid State Comm. **37**, 779
Echenique PM, Flores F and Ritchie RH, 1990: Solid State Physics **43**, 229
Eckstein W, 1987: Nucl. Instrum. Methods B **18**, 344
Eckstein W, 1988: Nucl. Instrum. Methods B **33**, 489
Eckstein W, 1991: *Computer Simulation of Ion-Solid Interactions* (Springer, Berlin)
Eckstein W and Biersack JP, 1984: Nucl. Instrum. Methods B **2**, 550
Eckstein W and Hou M, 1988: Nucl. Instrum. Methods B **31**, 386
Eckstein W and Hou M, 1991: Nucl. Instrum. Methods B **53**, 270
Eckstein W, Hackel S, Heinemann D and Fricke B, 1992: Z. Phys. D **24**, 171
Eklund EA, Bruinsma R, Rudnick J and Williams RS, 1991: Phys. Rev. Lett. **67**, 1759
Fallavier M, Kemmler J, Kirsch R, Poizat JC, Remillieux J, and Thomas JP, 1990: Phys. Rev. Lett. **65**, 621
Fano U and Lichten W, 1965: Phys. Rev. Lett. **14**, 627
Feller W, 1957: *An Introduction to Probability Theory and Its Applications, Vol. 1* (Wiley, New York, Second Edition)
Fermi E and Teller E, 1947: Phys. Rev. **72**, 399
Ferrell TL and Ritchie RH, 1977: Phys. Rev. B **16**, 115
Finnis MW and Heine V, 1974: J. Phys. F **4**, L37
Finnis MW and Sinclair JE, 1984: Phil. Mag. A**50**, 45
Firsov OB, 1957: Zh. Eksp. Teor. Fiz. **33**, 696 [Sov. Phys.-JETP **6** (1958) 534]
Firsov OB, 1959: Zh. Eksp. Teor. Fiz. **36**, 1517 [Sov. Phys.-JETP **36** (1959) 1076]
Flynn CP and Averback RS, 1988: Phys. Rev. B **38**, 7118
Foiles SM, 1987: Surface Sci. **191**, L779
Foiles SM, Baskes MI and Daw MS, 1986: Phys. Rev. B **33**, 7983
Gades H and Urbassek HM, 1992: Nucl. Instrum. Methods B **69**, 232
Garcia JD, Fortner RJ and Kavanagh TM, 1973: Rev. Mod. Phys. **45**, 111
Garrison BJ, 1986: Nucl. Instrum. Methods B**17**, 305

Garrison BJ, Winograd N, Lo DY, Tombrello TA, Shapiro MH, and Harrison DE, Jr, 1987: Surface Sci. **180**, L129
Garrison BJ, Winograd N, Deaven DM, Reiman CT, Lo DY, Tombrello TA, Harrison DE, Jr and Shapiro MH, 1988: Phys. Rev. B **37**, 7197
Gibson JB, Goland AN, Milgram M and Vineyard GH, 1960: Phys. Rev. **120**, 1229
Gombás P, 1956: *Handbuch der Physik*, edited by S. Fluegge (Springer, Berlin), Vol. XXXVI, pp. 109-231
Gordon RG and Kim YS, 1972: J. Chem. Phys. **56**, 3122
Grizzi O and Baragiola RA, 1987: Phys. Rev. A **35**, 135
Guellil AM and Adams JB, 1992: J. Mater. Res. **7**, 639
Hackel S, Fricke B, Heinemann D, Kolb D and Yang L, 1990: Report GSI-90-1, p. 165
Haggmark LG and Biersack JP, 1981: J. Nucl. Mater. **103/104**, 345
Harrison DE, Jr, 1981a: J. Appl. Phys. **52**, 1499
Harrison DE, Jr, 1981b: J. Appl. Phys. **52**, 4251
Harrison DE, Jr, 1983: Radiat. Eff. **70**, 1
Harrison DE, Jr, 1988: CRC Critical Reviews in Solid State and Materials Science **14**, S1
Harrison DE, Jr and Jakas MM, 1986a: Radiat. Eff. **99**, 637
Harrison DE, Jr and Jakas MM, 1986b: Nucl. Instrum. Methods B **15**, 25
Harrison DE, Jr and Webb RP, 1982: J. Appl. Phys. **53**, 4193
Harrison DE, Jr, Avouris P and Walkup R, 1987: Nucl. Instrum. Methods B **18**, 349
Hautala M, 1980: Radiat. Eff. **51**, 35
Hautala M, 1984: Phys. Rev. B **30**, 5010
Heinemann D, Rosen A and Fricke B, 1990: Phys. Scr. **41**, 692
Heinisch HL, Schiffgens JO and Schwartz DM, 1979: J. Nucl. Mater. **85/86**, 607
Hofer WO, 1991: *Sputtering by Particle Bombardment III*, edited by R Behrisch and K Wittmack (Springer, Berlin, etc) 15
Hoover WG, 1986: *Molecular Dynamics* (Springer, Berlin)
Hou M and Eckstein W, 1990: Phys. Rev. B **42**, 5959
Hou M and Eckstein W, 1992: J. Appl. Phys. **71**, 3975
Hou M and Robinson MT, 1976: Nucl. Instrum. Methods **132**, 641
Hou M. and Robinson MT, 1979: Appl. Phys. **18**, 381
Hou M, Eckstein W and Robinson MT, 1993: Nucl. Instrum. Methods B **82**, 234
Hsieh H and Averback RS, 1990: Phys. Rev. B **42**, 5365
Hsieh H, Diaz de la Rubia T, Averback RS and Benedek R, 1989: Phys. Rev. B **40**, 9986
Hsieh H, Averback RS, Sellers H and Flynn CP, 1992: Phys. Rev. B **45**, 4417
Igarashi M, Kanta K and Vitek V, 1991: Phil. Mag. B **63**, 603
Ishitani T, Shimase A and Hosaka S, 1983: Jap. J. Appl. Phys. **22**, 329
Jackson DP, 1973: Radiat. Eff. **18**, 185
Jackson DP, 1975: Can. J. Phys. **53**, 1513
Jacobsen KW, Nørskov JK and Puska MJ, 1987: Phys. Rev. B **35**, 7423
Jakas MM and Harrison DE, Jr, 1984: Phys. Rev. B **30**, 3573
Jakas MM and Harrison DE, Jr, 1985: Phys. Rev. B **32**, 2752
Johnson RA, 1991: Phil. Mag. A **63**, 865
Johnson RA and Oh DJ, 1989: J. Mater. Research **4**, 1195
Johnson RE and Schou J, 1993: K. Dan. Vidensk. Selsk. Mat. Fys. Medd. **43**, 403
Kaneko T, 1990a: Surface Science **236**, 203
Kaneko T, 1990b: Nucl. Instrum. Methods B **48**, 83
Kang HJ, Kawatoh E and Shimizu R, 1985: Jap. J. Appl. Phys. **24**, 1409
Karetta F and Urbassek HM, 1992: J. Appl. Phys. **71**, 5410
Karpuzov DS and Yurasova VE, 1971: Phys. Stat. Sol. **47**, 41

Kato M, Williams RS and Aono M, 1988: Nucl. Instrum. Methods B **33**, 462
Keinonen J, Kuronen A, Tikkanen P, Boerner HG, Jolie J, Ulbig S, Kessler EG, Nieminen RM, Puska MJ and Seitsonen AP, 1991: Phys. Rev. Lett. **67**, 3692
Kelly R, 1987: Nucl. Instrum. Methods B **18**, 388
Kessel QC and Everhart E, 1966: Phys. Rev. **146**, 16
Khor KE and Das Sarma S, 1987: Phys. Rev. B **36**, 7733
Kinchin GH and Pease RS, 1955a: J. Nucl. Energy **1**, 200
Kinchin GH and Pease RS, 1955b: Rep. Prog. Phys. **18**, 1
Kirsanov VV and Musin NN, 1990: Physics Lett. A **143**, 420
Kirsanov VV and Musin NN, 1991: Physics Lett. A **153**, 493
Klein KM, Park C and Tasch AF, 1990: Appl. Phys. Lett. **57**, 2701
Kwon I, Biswas R, Grest GR and Soukoulis CM, 1990: Phys. Rev. B **41**, 3678
Landman U, Hill RN and Mostoller M, 1980: Phys. Rev. B **21**, 448
Lehmann C and Sigmund P, 1966: Phys. Stat. Sol. **16**, 507
Leibfried G, 1958: Nukleonik **1**, 57
Leibfried G, 1965: *Bestrahlungseffekte in Festkörpern* (Teubner, Stuttgart) 153
Lennard WN, Xia Y and Geissel H, 1992: Nucl. Instrum. Methods B **67**, 44
Lichten W, 1967: Phys. Rev **164**, 131
Lichten W, 1980: J. Phys. Chem. **84**, 2102
Lindhard J and Scharff M, 1961: Phys. Rev. **124**, 128
Lindhard J, Nielsen V, Scharff M and Thomsen PV, 1963: K. Dan. Vidensk. Selsk. Mat. Fys. Medd. **33**, no. 10
Lindhard J, Nielsen V and Scharff M, 1968: K. Dan. Vidensk. Selsk. Mat. Fys. Medd. **36**, no. 10
Lo DY, Shapiro MH, Tombrello TA, Garrison BJ and Winograd N, 1987: Materials Research Society Symposia Proceedings **74**, 449
Lo DY, Tombrello TA, Shapiro MH, Garrison BJ, Winograd N and Harrison DE, Jr, 1988: J. Vac. Sci. Technol. A **6**, 708
Logan LR, Murthy CS and Srinivasan GR, 1992: Phys. Rev. A, **46**, 5754
Loisel B, Lapujoulade J and Pontikis V, 1991: Surface Sci. **256**, 247
Lu CC, Carlson TA, Malik FB, Tucker TC and Nestor C W, Jr, 1971: Atomic Data **3**, 1
Mashkova ES and Molchanov VA, 1989: Radiat. Eff. **108**, 307
Mazzone AM, 1988: Nucl. Instrum. Methods B **33**, 776
Merkle KL and Jaeger W, 1981: Phil. Mag. **44**, 741
Michely T and Comsa G, 1991: Phys. Rev. B **44**, 8411
Michely T and Comsa G, 1993: Nucl. Instrum. Methods B **82** 207
Michely T, Besocke KH and Comsa G, 1990: Surface Sci. Lett. **230**, L135
Mikkelsen HH, Meibom A and Sigmund P, 1992: Phys. Rev. A, **46**, 7012
Molière G, 1947: Z. Naturforsch. **2a**, 133
Mowrey RC, Brenner DW, Dunlap BI, Mintmire JW, and White CT, 1991: J. Phys. Chem. **95**, 7138
Mueller K-H, 1987: J. Appl. Phys. **61**, 2516
Murthy CS and Srinivasan G R, 1993: Phys. Rev. B, **47**, 1256
Nakagawa ST, 1990: Radiat. Eff. **112**, 1
Nakagawa ST, 1991: Radiat. Eff. **116**, 21
Nakagawa ST and Yamamura Y, 1988: Radiat. Eff. **105**, 239
Nieminen RM, 1993: K. Dan. Vidensk. Selsk. Mat. Fys. Medd. **43**, 81
Norgett MJ, Robinson MT and Torrens IM, 1975: Nucl. Engineer. Design **33**, 50
O'Connor DJ and Biersack JP, 1986: Radiat. Eff. **62**, 14
Oen OS and Robinson MT, 1976: Nucl. Instrum. Methods **132**, 647
Oliva A, Kelly R and Falcone G, 1987: Nucl. Instrum. Methods B **19/20**, 101

Pan Z, 1992: Nucl. Instrum. Methods B **66**, 325
Pan Z and Hou M, 1992: Nucl. Instrum. Methods B **67**, 401
Pan Z and Sigmund P, 1990: Nucl. Instrum. Methods B **51**, 344
Pasianot R and Savino EJ, 1992: Phys. Rev. B **45**, 12704
Pelletier JD, Shapiro MH and Tombrello TA, 1992: Nucl. Instrum. Methods B **67**, 296
Proennecke S, Caro A, Victoria M, Diaz de la Rubia T and Guinan MW, 1991: J. Mater. Res. **6**, 483
Reimann CT, 1993: K. Dan. Vidensk. Selsk. Mat. Fys. Medd. **43**, 351
Robinson MT, 1981: *Sputtering by Particle Bombardment I*, edited by R Behrisch (Springer, Berlin) 74
Robinson MT, 1983: J. Appl. Phys. **54**, 2650
Robinson MT, 1989: Phys. Rev. B **40**, 10717
Robinson MT, 1990: Nucl. Instrum. Methods B **48**, 408
Robinson MT, 1992a: MARLOWE User's Guide (Version 13), unpublished
Robinson MT, 1992b: Nucl. Instrum. Methods B **67**, 396
Robinson MT, 1992c: unpublished calculations
Robinson MT, 1993: Radiat. Eff, to be published
Robinson MT and Oen OS, 1982: J. Nucl. Mater. **110**, 147
Robinson MT and Torrens IM, 1974: Phys. Rev. B **9**, 5008
Ruzic DN, 1990: Nucl. Instrum. Methods B **47**, 118
Ruzic DN and Chiu HK, 1989: J. Nucl. Mater. **162-164**, 904
Sabelli NH, Kantor M, Benedek R and Gilbert TL, 1978: J. Chem. Phys. **68**, 2767
Sabelli NH, Benedek R and Gilbert TL, 1979: Phys. Rev. A **20**, 677
Scherzer BMU, 1983: *Sputtering by Particle Bombardment II*, edited by R Behrisch (Springer, Berlin) 271
Schlaug RN, 1965: Thesis, University of California, Berkeley (University Microfilms, Inc, Ann Arbor, Michigan, 1966)
Schwartz DM, Schiffgens JO, Doran DG, Odette GR and Ariyasu RG, 1976: *Computer Simulation for Materials Applications*, edited by RJ Arsenault, JR Beeler, Jr and JA Simmons. Nucl. Metall. **20**, 75
Shapiro MH and Fine J, 1989: Nucl. Instrum. Methods B **44**, 43
Shapiro MH and Tombrello TA, 1987: Nucl. Instrum. Methods B **18**, 355
Shapiro MH and Tombrello TA, 1990a: Phys. Rev. Lett. **65**, 92
Shapiro MH and Tombrello TA, 1990b: Nucl. Instrum. Methods B **48**, 557
Shapiro MH and Tombrello TA, 1991a: Nucl. Instrum. Methods B **58**, 161
Shapiro MH and Tombrello TA, 1991b: Nucl. Instrum. Methods B **62**, 35
Shapiro MH and Tombrello TA, 1992a: Phys. Rev. Lett. **68**, 1613
Shapiro MH and Tombrello TA, 1992b: Nucl. Instrum. Methods B **66**, 317
Shapiro MH, Tombrello TA and Harrison DE, Jr, 1988: Nucl. Instrum. Methods B **30**, 152
Shulga VI, 1980: Radiat. Eff. **51**, 1
Shulga VI, 1982: Radiat. Eff. **62**, 237
Shulga VI, 1983: Radiat. Eff. **70**, 65
Shulga VI, 1991: Nucl. Instrum. Methods B **58**, 422
Shulga VI and Sigmund P, 1990: Nucl. Instrum. Methods B **47**, 236
Shulga VI and Sigmund P, 1991: Nucl. Instrum. Methods B **62**, 23
Shulga VI, Vicanek M and Sigmund P, 1989: Phys. Rev. A **39**, 3360
Sigmund P, 1981: *Sputtering by Particle Bombardment I*, edited by R Behrisch (Springer, Berlin) 9
Sigmund P, 1987a: Nucl. Instrum. Methods B **18**, 375
Sigmund P, 1987b: Nucl. Instrum. Methods B **27**, 1

Sigmund P, 1989: J. Phys. (Paris), Coll. C-2 **50**, 175
Sigmund P, 1991: *Interaction of Charged Particles with Solids and Surfaces*, NATO ASI Series, Vol. 271, edited by A Gras-Marti et al. (Plenum, New York), 73
Sigmund P and Lam NQ, 1993: K. Dan. Vidensk. Selsk. Mat. Fys. Medd. **43**, 255
Sigmund P, Robinson MT, Baskes MI, Hautala M, Cui FZ, Eckstein W, Yamamura Y, Hosaka S, Ishitani T, Shulga VI, Harrison DE, Jr, Chakarov IR, Karpuzov DS, Kawatoh E, Shimizu R, Valkealahti S, Nieminen RM, Betz G, Husinsky W, Shapiro MH, Vicanek M and Urbassek HM, 1989: Nucl. Instrum. Methods B **36**, 110
Smith R, 1992: Nucl. Instrum. Methods B **67**, 335
Smith R and Harrison DE, Jr, 1989: Phys. Rev. B **40**, 2090
Smith R and Webb RP, 1991: Nucl. Instrum. Methods B **59/60**, 1378
Smith R and Webb RP, 1992: Nucl. Instrum. Methods B **67**, 373
Smith R and Webb RP, 1993: Proc. Roy. Soc. Lond. A **441**, 475
Smith R, Harrison DE, Jr and Garrison BJ, 1989: Phys. Rev. B **40**, 93
Smith R, Harrison DE, Jr and Garrison BJ, 1990: Nucl. Instrum. Methods B **46**, 1
Stansfield RA, Broomfield K and Clary DC, 1989: Phys. Rev. B **39**, 7680
Stillinger FH and Weber TA, 1985: Phys. Rev. B **31**, 5262
Stoneham AM, 1990: Nucl. Instrum. Methods B **48**, 389
Takeuchi W and Yamamura Y, 1983: Radiat. Eff. **71**, 51
Tersoff J, 1986: Phys. Rev. Lett. **56**, 632
Tersoff J, 1988a: Phys. Rev. B **37**, 6991
Tersoff J, 1988b: Phys. Rev. Lett. **61**, 2879
Tersoff J, 1988c: Phys. Rev. B **38**, 9902
Thompson DA, 1981: J. Appl. Phys. **52**, 982
Thompson MW, 1968: Phil. Mag. **18**, 377
Torrens IM, 1973: J. Phys. F **3**, 1771
Tsong IST and Bedrossian P, 1993: K. Dan. Vidensk. Selsk. Mat. Fys. Medd. **43**, 209
Tucker TC, Roberts LD, Nestor CW, Jr and Carlson TA, 1969: Phys. Rev. **178**, 998
Uhlenbeck GE and Ornstein LS, 1930: Phys. Rev. **36**, 823
Urbassek HM and Hofer WO, 1993: K. Dan. Vidensk. Selsk. Mat. Fys. Medd. **43**, 97
Valkealahti S and Nieminen RM, 1987: Nucl. Instrum. Methods B **18**, 365
van Midden HJP and Sasse AGBM, 1992: Phys. Rev. B **46**, 6020
Vicanek M and Urbassek HM, 1988: Nucl. Instrum. Methods B **30**, 507
Wang MC and Uhlenbeck GE, 1945: Rev. Mod. Phys. **17**, 323
Wax N, 1954: *Selected Papers on Noise and Stochastic Processes* (Dover, New York). Includes reprints of Chandrasekhar (1943), Uhlenbeck & Ornstein (1930) and Wang & Uhlenbeck (1945)
Webb RP, Harrison DE, Jr and Jakas MM, 1986: Nucl. Instrum. Methods B **15**, 1
Whitlow HJ and Hautala M, 1987: Nucl. Instrum. Methods B **16**, 370
Wilson WD, Haggmark LG and Biersack JP, 1977: Phys. Rev. B **15**, 2458
Wucher A and Garrison BJ, 1992a: Surface Sci. **260**, 257
Wucher A and Garrison BJ, 1992b: Phys. Rev. B **46**, 4855
Wucher A and Garrison BJ, 1993: Nucl. Instrum. Methods B **82**, 352
Wucher A, Watgen M, Moessner C, Oechsner O and Garrison BJ, 1992: Nucl. Instrum. Methods B **67**, 531
Yamamura Y, 1982: Nucl. Instrum. Methods **194**, 515
Yamamura Y, 1988: Nucl. Instrum. Methods B **33**, 493
Yamamura Y, 1990: Nucl. Instrum. Methods B **45**, 707
Yamamura Y, 1991: Nucl. Instrum. Methods B **62**, 181

Yamamura Y and Muramoto T, 1993: Nucl. Instrum. Methods B, to be published
Yamamura Y and Muraoka K, 1989: Nucl. Instrum. Methods B **42**, 175
Yamamura Y and Takeuchi W, 1987: Nucl. Instrum. Methods B **29**, 461
Yamamura Y, Moessner C and Oechsner O, 1987a: Radiat. Eff. **103**, 25
Yamamura Y, Moessner C and Oechsner O, 1987b: Radiat. Eff. **105**, 31
Yamamura Y, Yamada I and Takagi T, 1989: Nucl. Instrum. Methods B **37/38**, 902
Yu ML, 1991: *Sputtering by Particle Bombardment III*, edited by R Behrisch, and K Wittmaack (Springer, Berlin) 91
Yurasova VE and Eltekov VA, 1982: Vacuum **32**, 399
Ziegler JF, Biersack JP and Littmark U, 1985: *Stopping Powers and Ranges of Ions in Matter* (Pergamon, New York), pp. 25ff